Energetic particle transport in theory, modelling and experiments in magnetically confined plasmas

D. Zarzoso

Aix Marseille Univ, CNRS, Centrale Med, M2P2 UMR 7340, Marseille, France

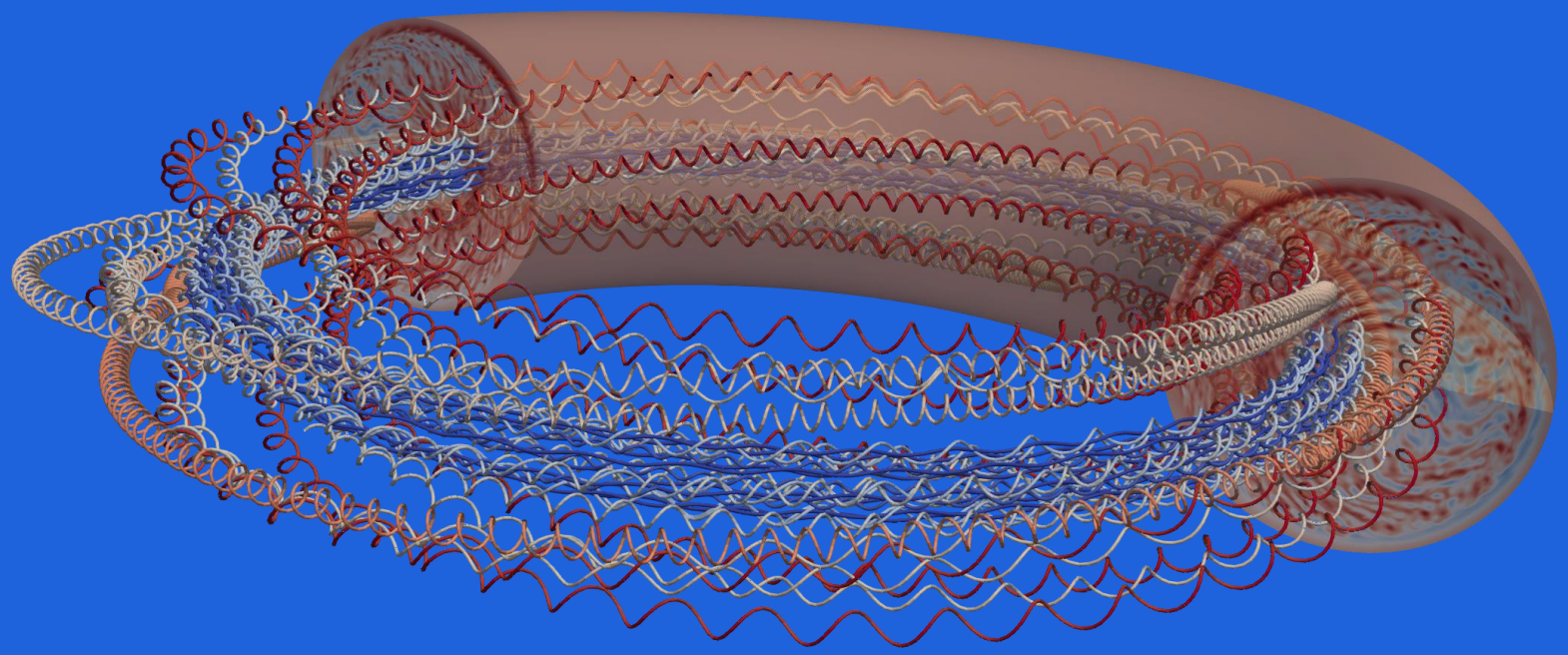

Acknowledgments

H. Betar, D. del-Castillo-Negrete, B. Clavier, I. Mavrogiannis, J. Varela-Rodriguez, L. Garcia G. Dif-Pradalier, V. Grandgirard, P. Donnel and X. Du

AIM4EP Project (ANR-21-CE30-0018), funded by the French National Research Agency (ANR)

Aix Marseille Université

Outline of the presentation

Fundamental physics of energetic particles in tokamaks and basics on transport

Toroidal Accelerated PArticle Simulator (TAPAS)

↪ Example of application to realistic experimental case

Non axi-symmetric modes, both static and rotating (tearing modes)

↪ Purely magnetic large scale $(m, n) = (2,1)$, $\omega \ll 0$

Ion-temperature gradient (ITG) driven turbulence

↪ Electrostatic with a broad spectrum (m, n, k_r)

Outline of the presentation

Fundamental physics of energetic particles in tokamaks and basics on transport

Toroidal Accelerated PArticle Simulator (TAPAS)

↪ Example of application to realistic experimental case

Non axi-symmetric modes, both static and rotating (tearing modes)

↪ Purely magnetic large scale $(m, n) = (2,1)$, $\omega \ll 0$

Ion-temperature gradient (ITG) driven turbulence

↪ Electrostatic with a broad spectrum (m, n, k_r)

The energies of energetic ions

- To keep the thermal plasma at constant temperature, a steady source of bulk plasma heating must be provided
- Auxiliary ion heating methods
  - Ion Cyclotron Range of Frequencies (ICRF) ~ 100 keV (minority heating) up to ~ 1 MeV (second, third harmonics and three-ion scheme)
  - Neutral Beam Injection (NBI) $\sim 20 - 180$ keV (positive ions, in most present devices) up to 870 keV (negative ions in LHD, JT-60U, ITER)
- Nuclear fusion reactions generate alpha particles at 3.5 MeV
- Need to be sufficiently well confined to transfer their energy to the thermal plasma
- Analysis of the range of energies from ~ 20 keV up to the 3.5 MeV birth energy of alpha particles
- Many more details on energetic particles can be found in [Salewski NF 2025] (and 1336 references therein)

Orbit width of EP ≫ orbit of thermal ions

The motion of a charged particle in a tokamak is quasi-periodic around the magnetic field lines and in the poloidal and toroidal directions ⟶ we define a set of action-angle variables

⇒ $\boldsymbol{J}$ are motion invariants associated to the three periodic directions

$$J_1 = -\frac{m\mu}{eZ} \qquad \underbrace{J_2 \to E = E_\parallel + E_\perp = \frac{mv_\parallel^2}{2} + \mu B \qquad J_3 \equiv P_\varphi = -eZ\psi + m\frac{B_\varphi}{B}v_\parallel}_{\text{Deviation from the flux surfaces} \longrightarrow \text{Orbit width}}$$

$$\Delta_{passing} \sim 2q\rho_i \qquad \Delta_{trapped} \sim 2q\rho_i/\sqrt{\epsilon}$$

$\Delta_{trapped,\alpha} \sim 15\%$ to 50% of the minor radius in ITER and JET, respectively

Orbit width of EP ≫ orbit of thermal ions

The motion of a charged particle in a tokamak is quasi-periodic around the magnetic field lines and in the poloidal and toroidal directions ⟶ we define a set of action-angle variables

⇒ $\boldsymbol{J}$ are motion invariants associated to the three periodic directions

$$J_1 = -\frac{m\mu}{eZ} \qquad \underbrace{J_2 \to E = E_\parallel + E_\perp = \frac{mv_\parallel^2}{2} + \mu B \qquad J_3 \equiv P_\varphi = -eZ\psi + m\frac{B_\varphi}{B}v_\parallel}$$

Deviation from the flux surfaces ⟶ Orbit width

$$\Delta_{passing} \sim 2q\rho_i \qquad \Delta_{trapped} \sim 2q\rho_i/\sqrt{\epsilon}$$

$\Delta_{trapped,\alpha} \sim 15\%$ to 50% of the minor radius in ITER and JET, respectively

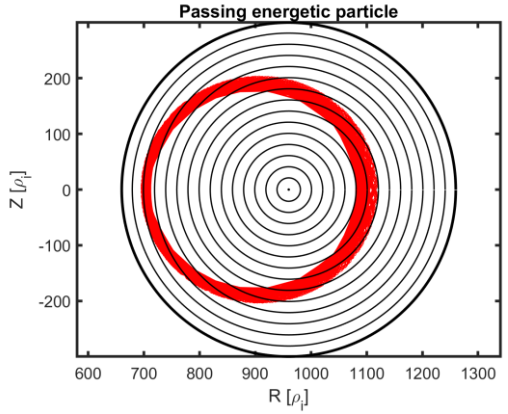

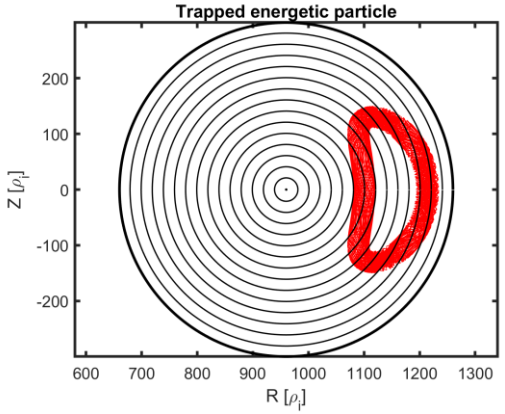

Characteristic frequencies of α particles

Linear resonance: $\omega - n_2\Omega_2 - n_3\Omega_3 = 0$ (NL resonances only for large perturbations [Sanchis PPCF 2018, Kramer PRL 2012])

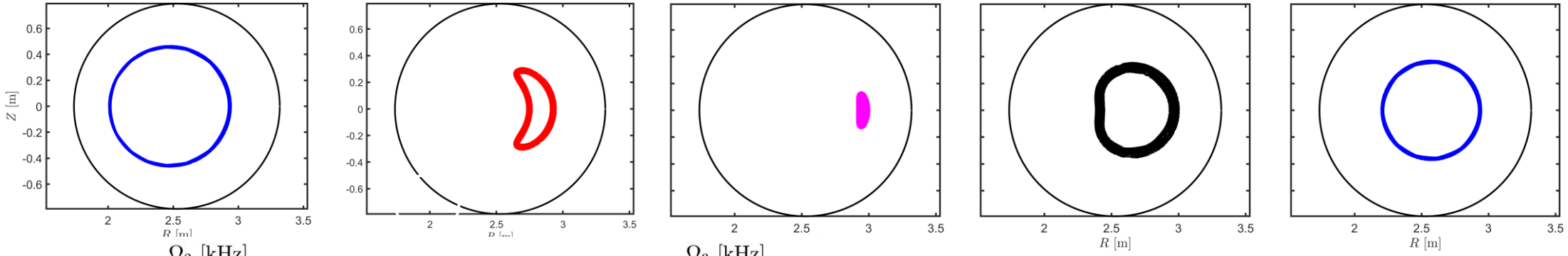

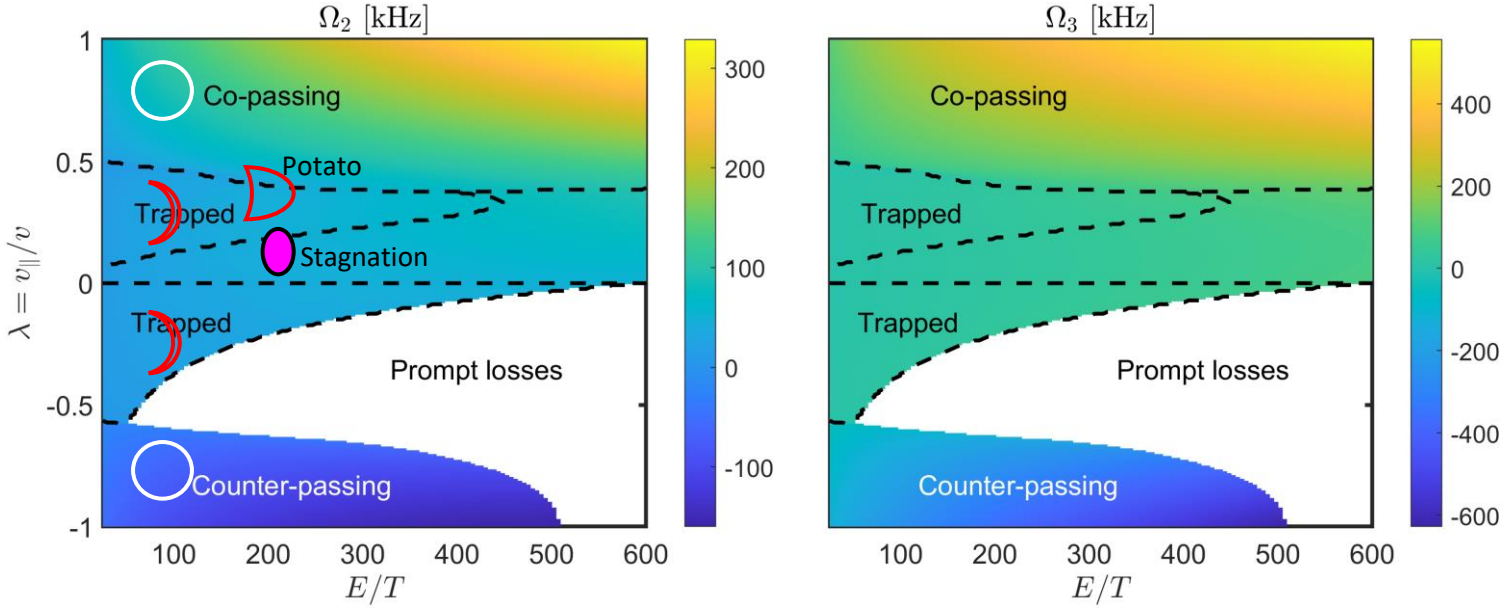

E_α =	500 keV	1 MeV	3,5 MeV
$\Omega_{2,passing}$	130 kHz	180 kHz	340 kHz
$\Omega_{3,passing}$	260 kHz	360 kHz	680 kHz
$\Omega_{2,trapped}$	50 kHz	70 kHz	130 kHz
$\Omega_{3,trapped}$	10 kHz	20 kHz	60 kHz

From micro- to macroscopic transport

Microscopic random kicks → Macroscopic transport

↪ Statistics of micro-scale motion governs the nature of transport

$$D_x = \frac{1}{2}\frac{d\sigma_x^2}{dt} = \frac{1}{2}\frac{d}{dt}\langle(\Delta x - \langle\Delta x\rangle)^2\rangle$$

Kick = i.i.d. random variables x_i → Total displacement $x = \sum x_i$

✓ $\langle x_i\rangle, \langle x_i^2\rangle < \infty \implies \sum x_i \sim$ Gaussian PDF ≡ Diffusion

✓ $\langle x_i\rangle, \langle x_i^2\rangle \longrightarrow \infty \implies \sum x_i \sim$ Lévy PDF ≡ Anomalous diffusion

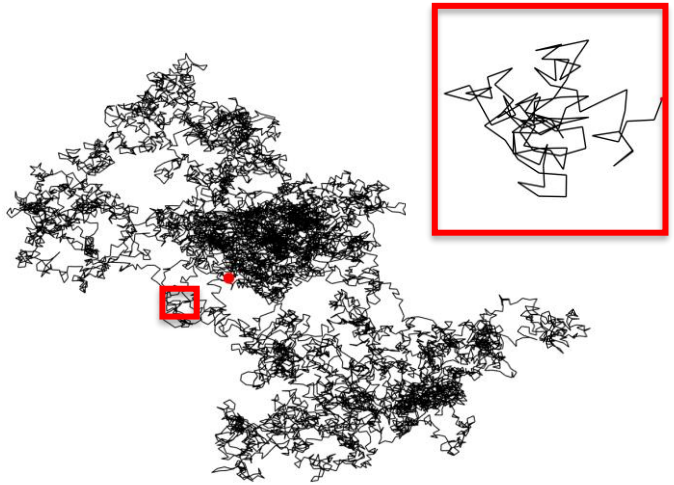

$\langle\Delta x^2\rangle \sim t$

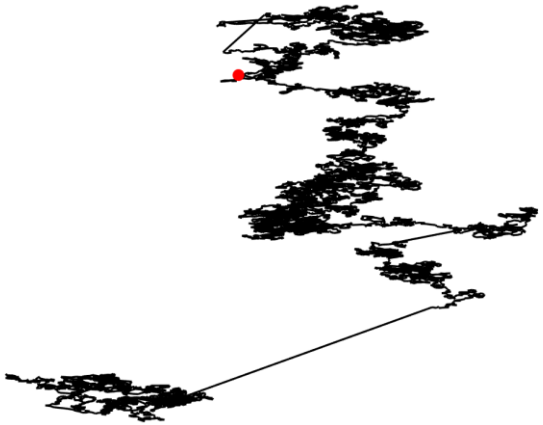

$\langle\Delta x^2\rangle \sim t^\gamma, \gamma \neq 1$

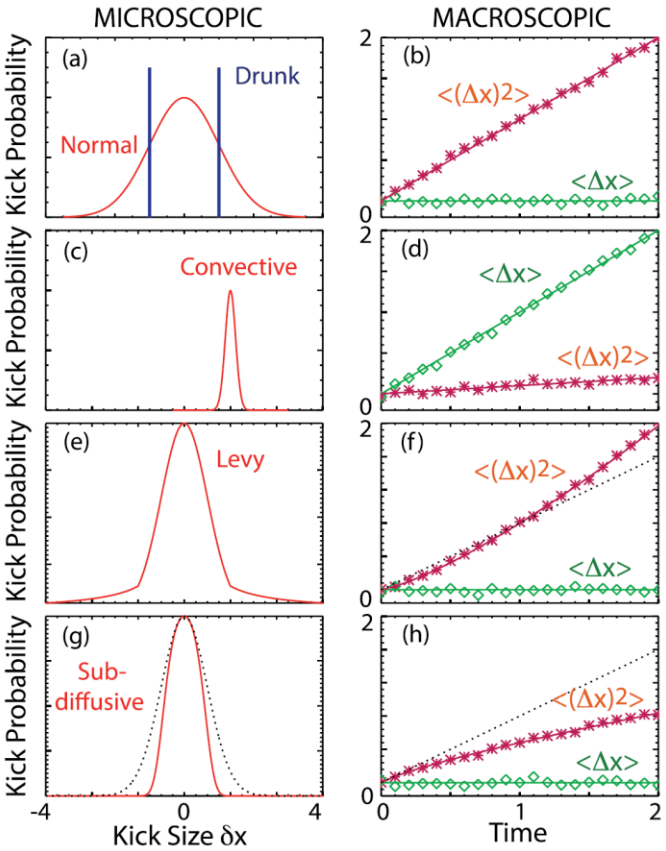

From [Heidbrink PoP 2020]

Diffusion $\longrightarrow$ Exponential decay $P_{exit} \sim e^{-\mu_e t}$

- The simplest model for radial transport in toroidal geometry

The radial diffusion equation for the particle density $\frac{\partial n}{\partial t} = \frac{\chi}{r}\frac{\partial}{\partial r}\left(r\frac{\partial n}{\partial r}\right)$

- Probability of exit time $P_{exit}(t)$ and the mean exit time $\langle t_{exit}\rangle$ exhibit the local diffusive scalings

$$\langle t_{exit}\rangle = \frac{\pi a^2}{4\chi} \qquad P_{exit} \sim \frac{1}{\langle t_{exit}\rangle} e^{-\frac{3t}{2\langle t_{exit}\rangle}}$$

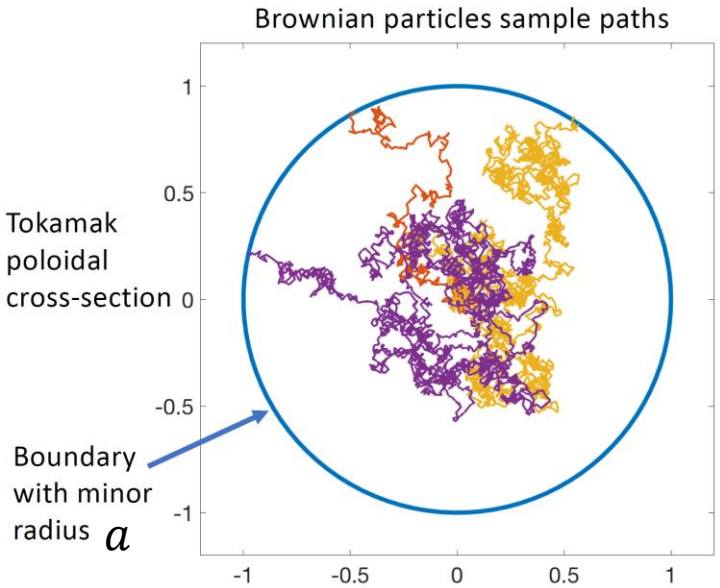

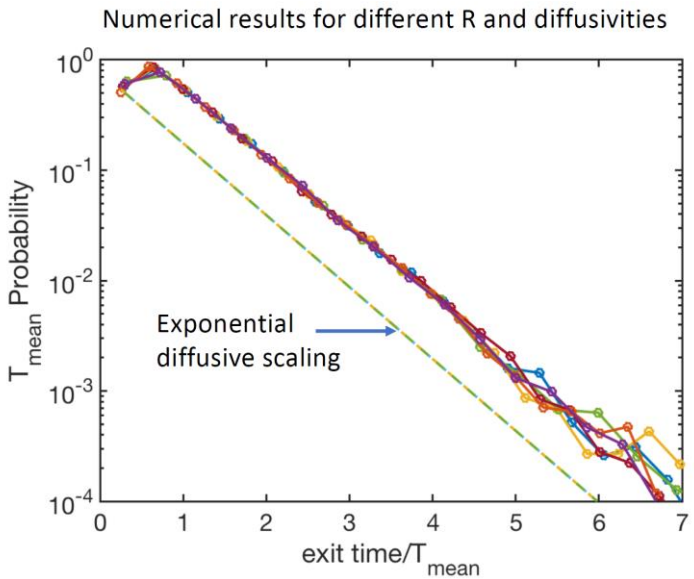

Outline of the presentation

Fundamental physics of energetic particles in tokamaks and basics on transport

Toroidal Accelerated PArticle Simulator (TAPAS)

↪ Example of application to realistic experimental case

Non axi-symmetric modes, both static and rotating (tearing modes)

↪ Purely magnetic large scale $(m, n) = (2,1)$, $\omega \ll 0$

Ion-temperature gradient (ITG) driven turbulence

↪ Electrostatic with a broad spectrum (m, n, k_r)

TAPAS to study the transport of EP

- **T**oroidal **A**ccelerated **PA**rticle **S**imulator
- Guiding-centre (GC, 5D) & full-orbit (FO, 6D)
  - ↪ GC solved using RK4
  - ↪ FO solved using Boris algoritm
- Collision operator (deterministic + stochastic)
- Source of energy and particles (NBI)
- Realistic geometries
- Accelerated on GPU, including the 3D B-spline interpolations
- Allows for large number of particles ($\sim 10^9$)
- Coupled to external codes (FAR3d, GYSELA) to use 3D perturbations
- Applied to DIII-D (and currently to JET discharges).

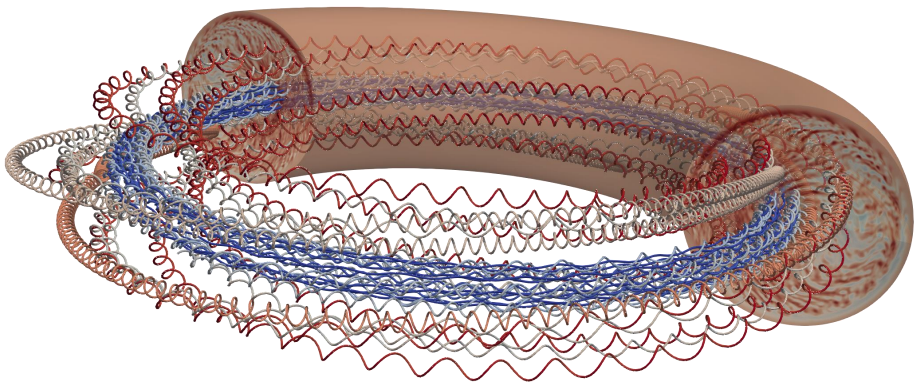

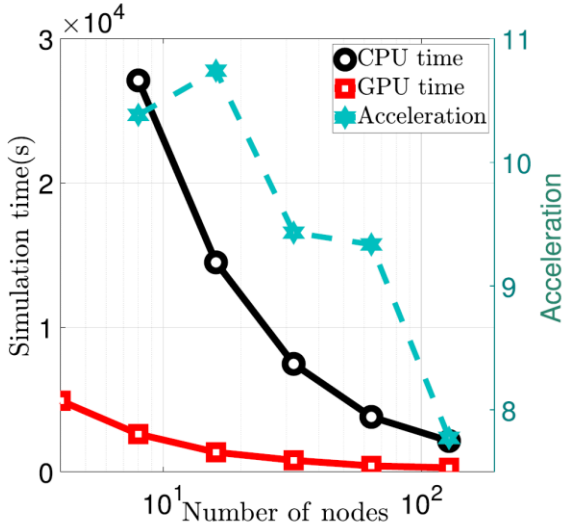

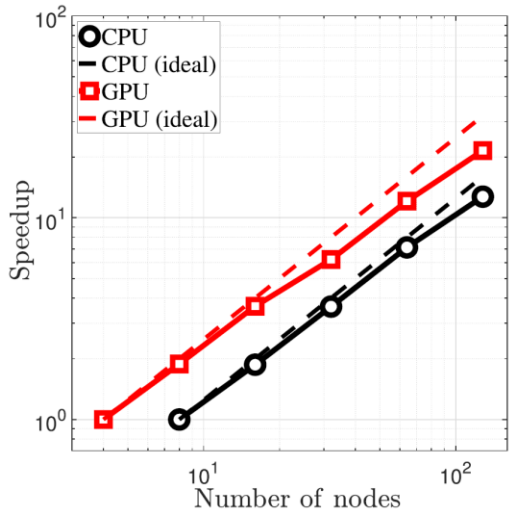

[H. Betar, D. Zarzoso *et al Nuclear Fusion* 2024]

Coupling with FAR3d code to model EP transport

FAR3d solves the reduced MHD equations for the thermal plasma and the density and parallel velocity equations for the EP population using a two-pole closure model [Varela Frontiers in Physics 2024]

Applied to the discharge #159243 of DIII-D with $\beta_{EP} = 3\%$ using the modes $n = 0\ (m = -14, \dots, 14), n = 3\ (m = -20, \dots, 20), n = 6\ (-52, \dots, 52)$

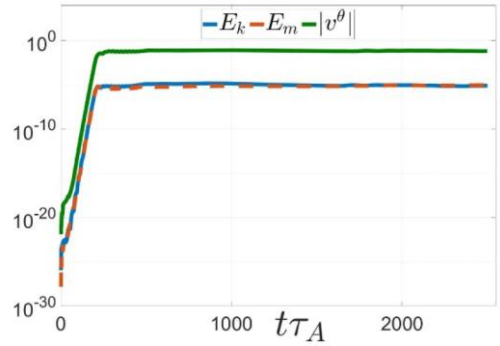

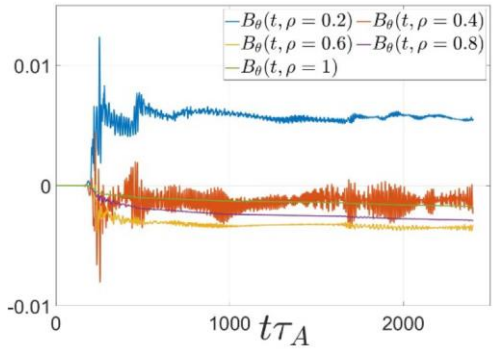

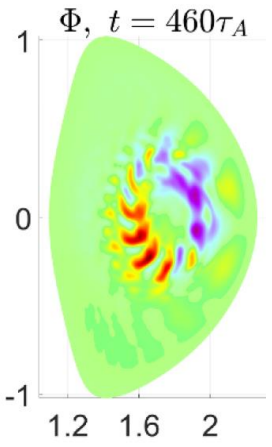

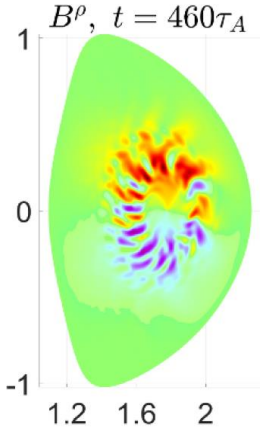

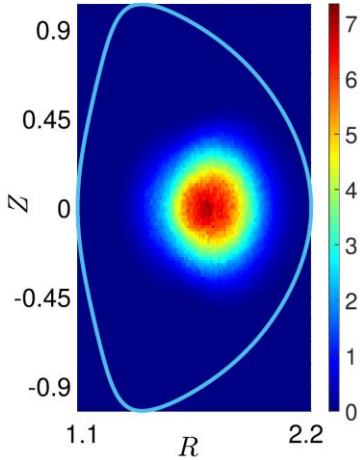

RSAE excited by passing Deuterium (tangential NBI), with presence of zonal flows and bursty behaviour in the inner part of the plasma, correlated with the location of the Alfvén activity

Monoenergetic beam exhibits losses near the prompt losses region [Betar NF 2024]

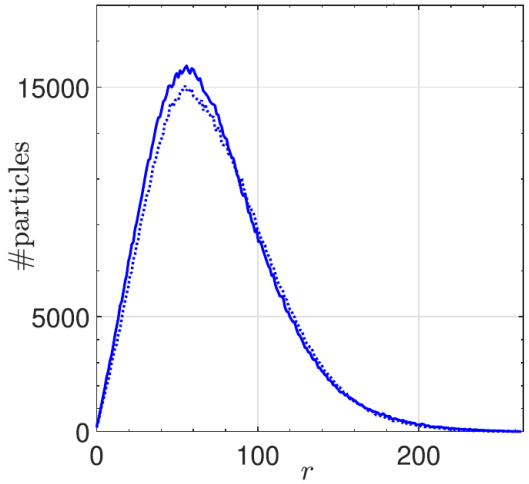

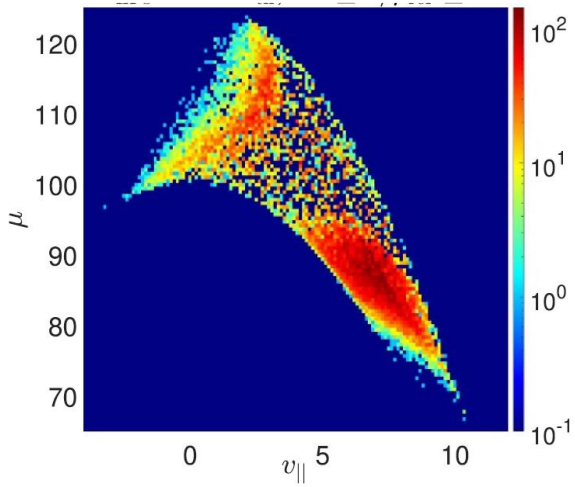

Outline of the presentation

Fundamental physics of energetic particles in tokamaks and basics on transport

Toroidal Accelerated PArticle Simulator (TAPAS)

↪ Example of application to realistic experimental case

Non axi-symmetric modes, both static and rotating (tearing modes)

↪ Purely magnetic large scale $(m, n) = (2,1)$, $\omega \ll 0$

Ion-temperature gradient (ITG) driven turbulence

↪ Electrostatic with a broad spectrum (m, n, k_r)

Magnetic islands → EP transport and losses

- Tearing mode
  - Large scale MHD mode driven unstable by the radial gradient of the plasma current (q-profile)
  - Modifies the magnetic topology (presence of magnetic islands)
  - Degrades confinement and can result in disruptions [Sauter PoP1997]
- Can have negative impact on energetic particle confinement [Mynick PoFB1993, Carolipio NF2002, Garcia-Muñoz NF2007, Yu AIPAdvances2021, Zarzoso PPCF 2022, Martinell PoP 2025]
  - Observed experimentally in TFTR, DIII-D, AUG and EAST.
  - Confirmed numerically using ORBIT
  - Chaos in EP trajectories

  ↪ Significant losses with tearing mode

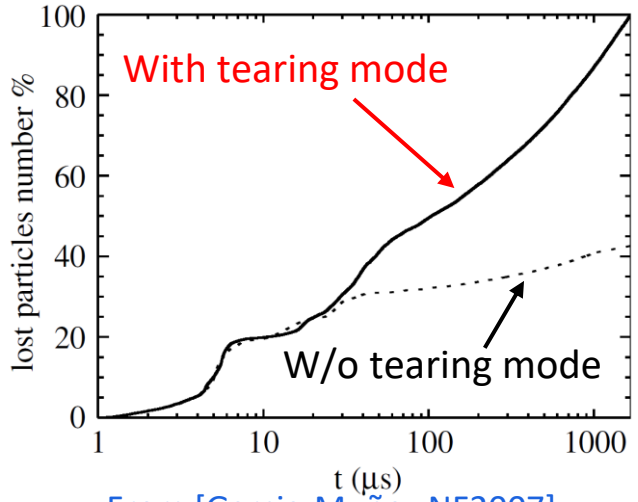

From [Garcia-Muñoz NF2007]

Transition to chaos

Trajectories of fusion-born α particles (3.5 MeV) integrated using GC approach (and FO approach for comparison)

Islands in trajectory Poincaré maps are distorted following the orbit drift of particles.

Existence of overlap of main and secondary islands as the orbit drift increases, as reported in [Mynick PoFB1993, Carolipio NF2002, Garcia-Muñoz NF2007].

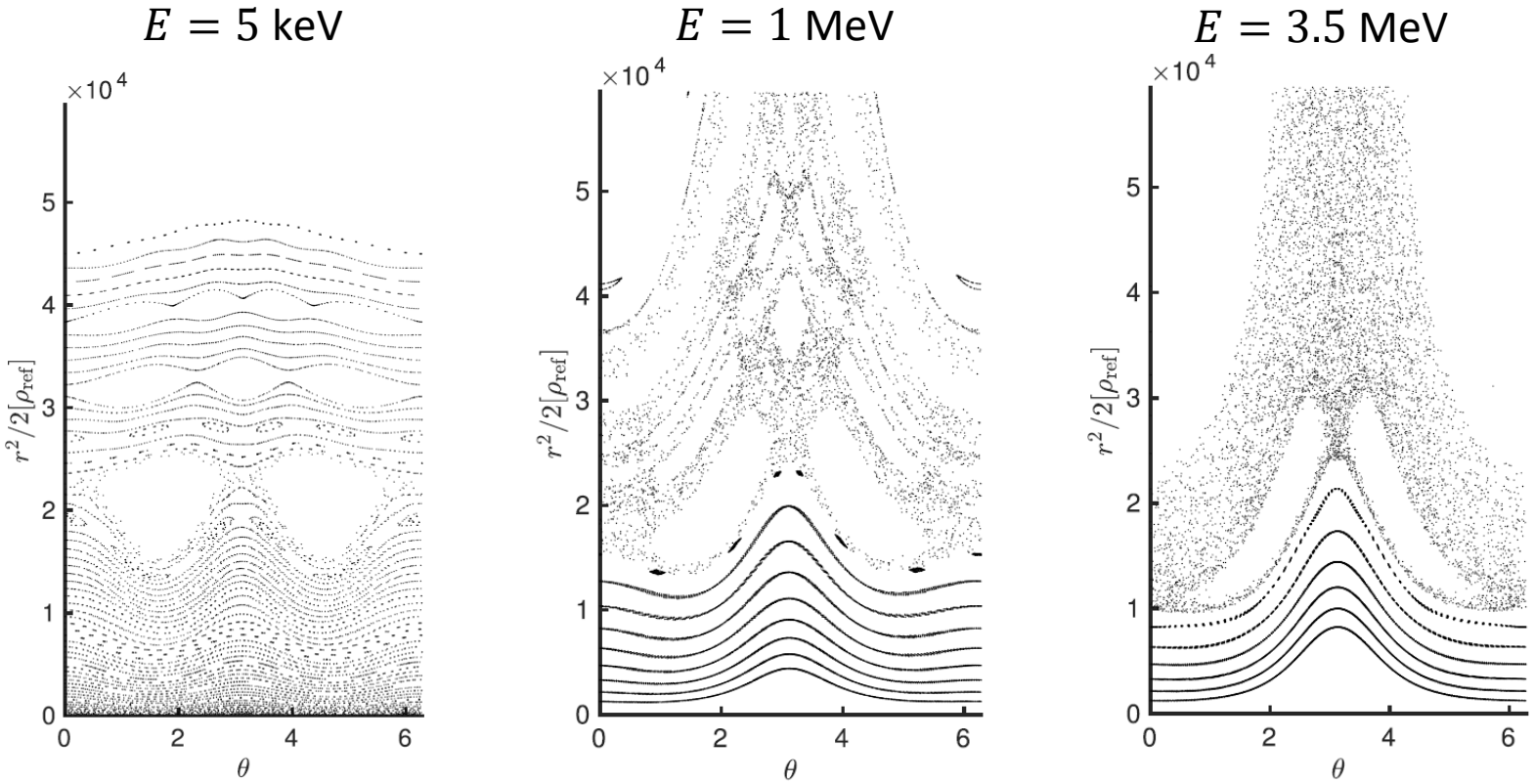

Mainly passing particles are affected by the magnetic island

Losses increase with the width of the island (as expected), more important for passing than for trapped particles

Significant losses, but less pronounced than in [Bonofiglo NF 2025], with mild stochasticity due to the absence of higher order harmonics and different initialization of α particle population.

Further analyses are required to assess the impact on the α confinement during the whole slowing-down process.

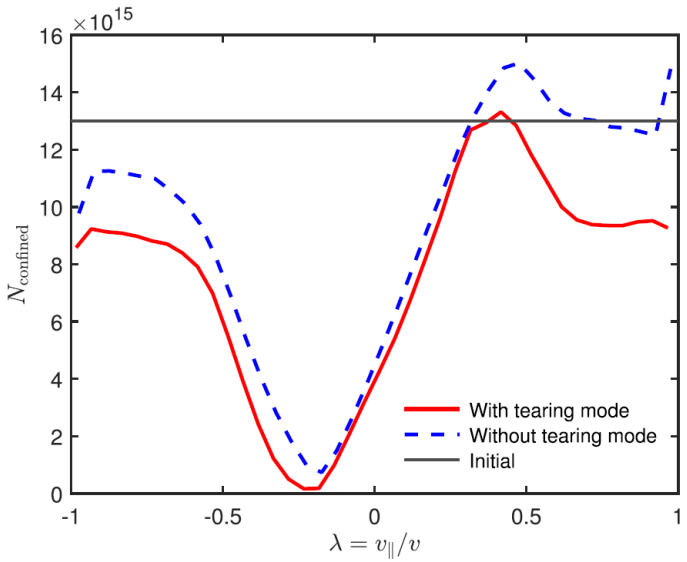

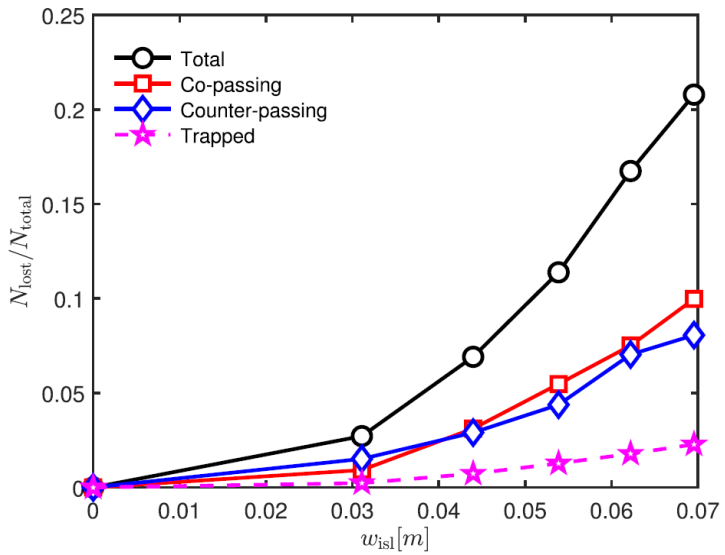

Magnetic island induced transport is non-diffusive

Non-exponential decay of the PDF of exit time → Non-diffusive transport
Algebraic decay depends on the class of particle and the amplitude of the perturbation, with an averaged exponent for all particles of $0.8 < \mu_e < 1.0$
Similar behaviour observed for oscillating radial electric field [Zarzoso&del-Castillo-Negrete JPP2020] linked to Lévy flights ⟶ Difficulty to model the transport using simple diffusion models

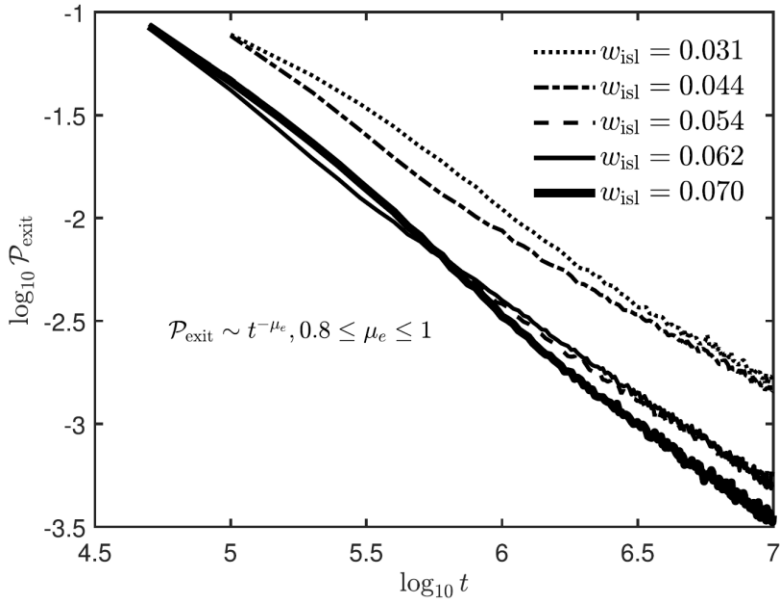

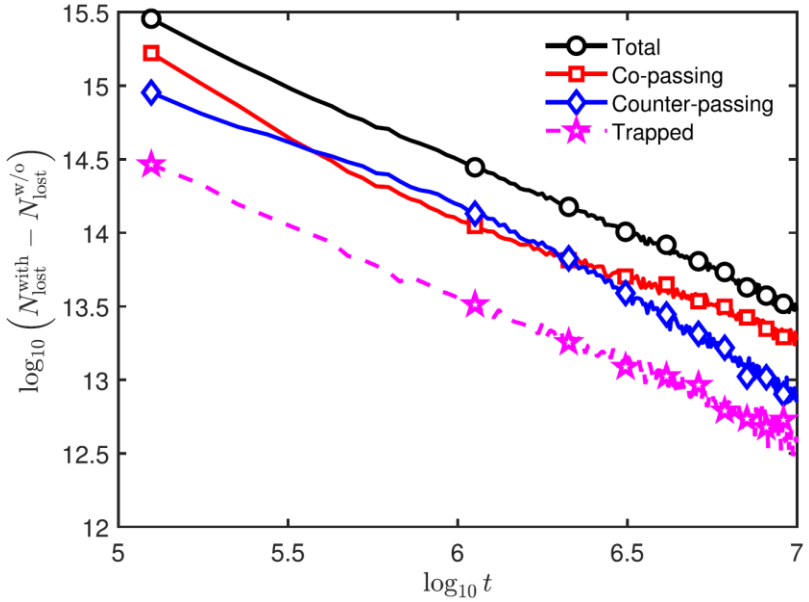

Impact of rotation on the losses of particles

A magnetic island rotates in the plasma frame, except when it is locked

We introduce a rotation in the ion direction ($\omega_{island} > 0$) or in the opposite direction ($\omega_{island} < 0$)

Losses are increased for trapped particles and for co-passing particles for $\omega_{island} > 0$

Losses are reduced for counter-passing particles for $\omega_{island} < 0$

$\omega_{island} < 0$

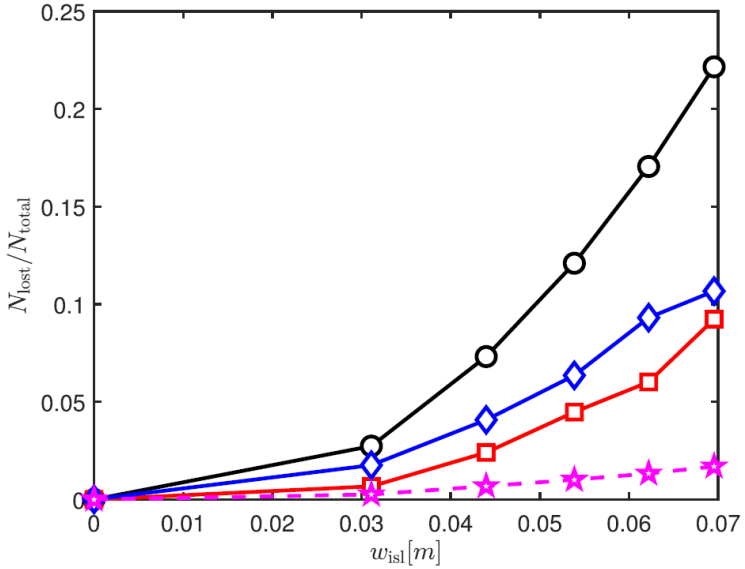

$\omega_{island} > 0$

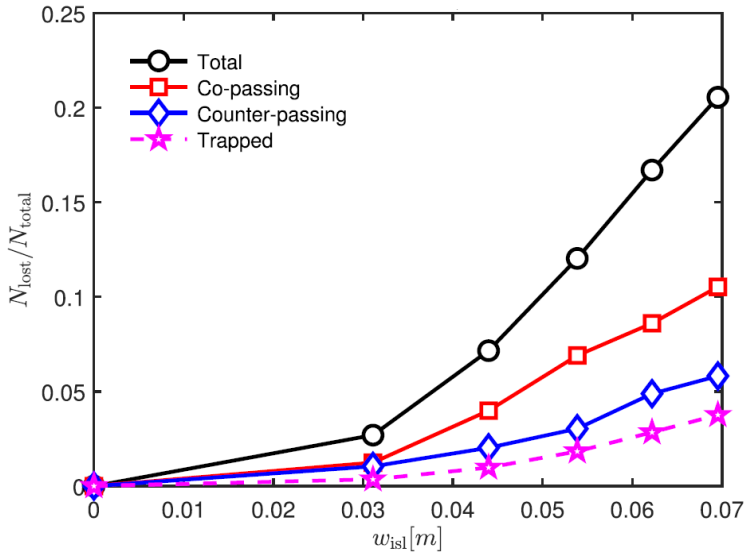

Effects of resonances on the losses of particles

Resonances mainly present in the co- and counter-passing regions → Losses of passing particles are more pronounced

Negative rotation frequency → Resonances are pushed towards the inner part of the counter-passing region and towards the outer part of the co-passing region ⇒ Counter-passing particles are more affected by islands with $\omega_{island} < 0$

Positive rotation frequency → Resonances are pushed towards the trapped region ⇒ Trapped particles are more affected by islands with $\omega_{island} > 0$

$\omega_{island} < 0$

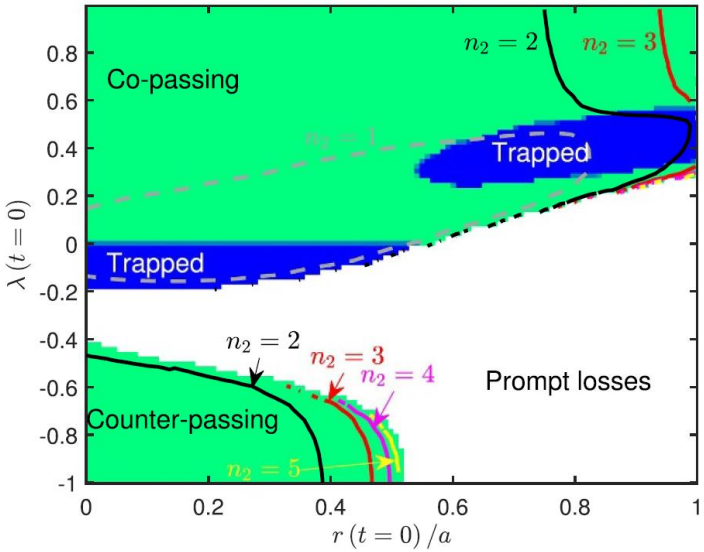

$\omega_{island} = 0$

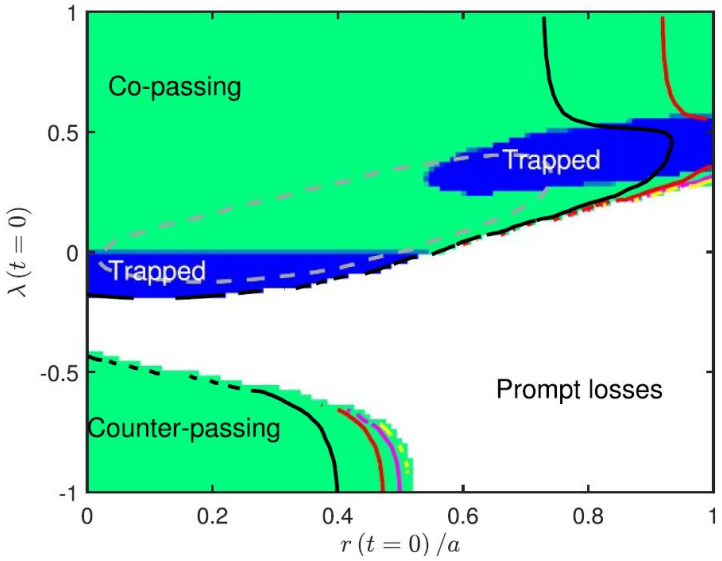

$\omega_{island} > 0$

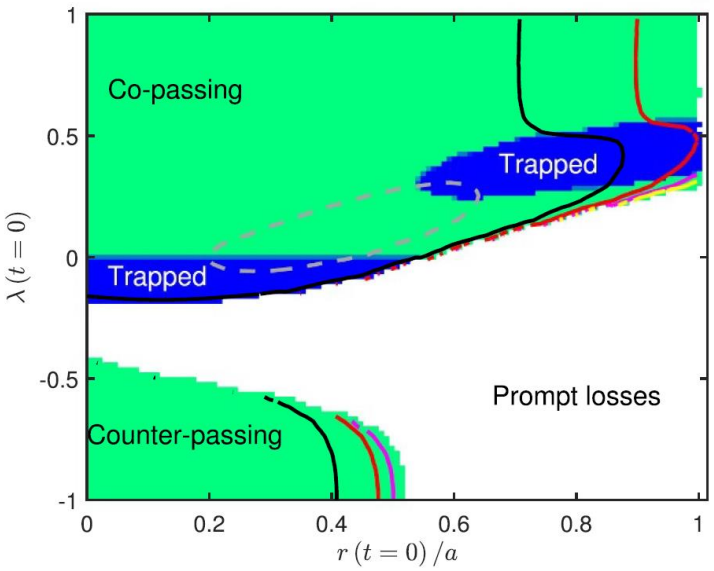

Effects of resonances on the losses of particles

Resonances mainly present in the co- and counter-passing regions → Losses of passing particles are more pronounced

Negative rotation frequency → Resonances are pushed towards the inner part of the counter-passing region and towards the outer part of the co-passing region ⇒ Counter-passing particles are more affected by islands with $\omega_{island} < 0$

Positive rotation frequency → Resonances are pushed towards the trapped region ⇒ Trapped particles are more affected by islands with $\omega_{island} > 0$

The location of the resonances is correlated with the probability of losses, similar to [Sanchis PPCF 2018]

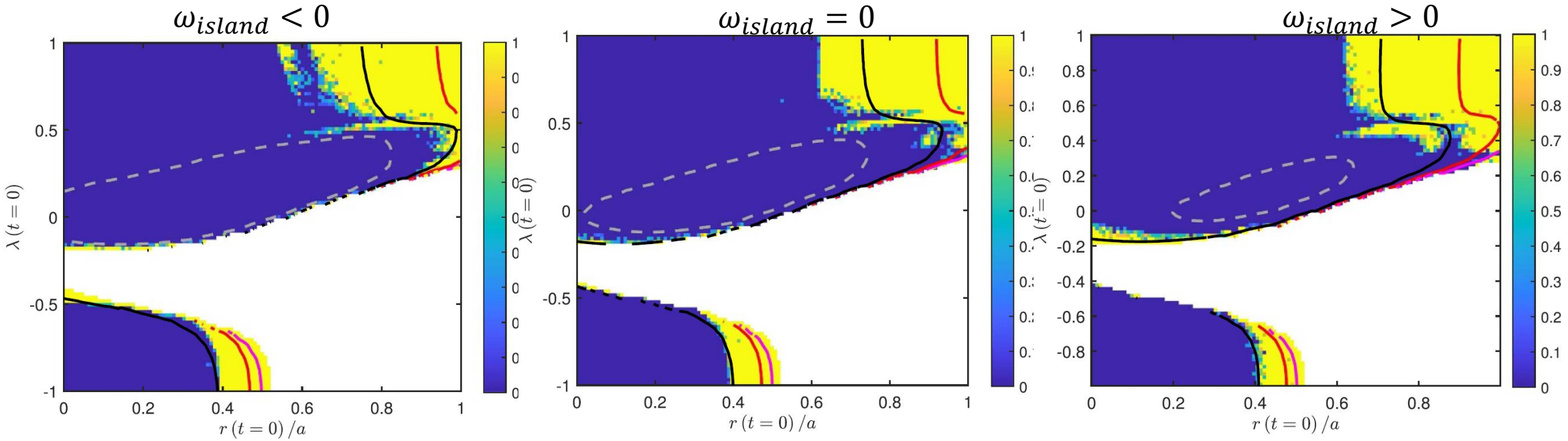

Finite Larmor radius effects through full-orbit simulations

Need to perform simulations in full-orbit, following [Martinell PoP 2025]

↪ Energies characteristic of NBI heating (10 keV and 50 keV)

↪ Similar behaviour due to island rotation (resonances effect)

↪ But GC less sensitive to magnetic island rotation than FO

Finite Larmor radius effects through full-orbit simulations

Need to perform simulations in full-orbit, following [Martinell PoP 2025]

↪ Energies characteristic of NBI heating (10 keV and 50 keV)

↪ Similar behaviour due to island rotation (resonances effect)

↪ But GC less sensitive to magnetic island rotation than FO

In TAPAS, full-orbit seems to produce less transport than GC (α particles at 3.5 MeV with an island width $\sim\rho_\alpha$)

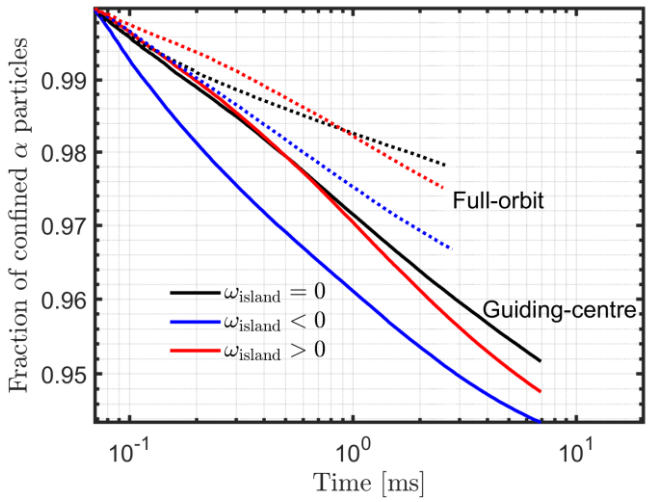

Finite Larmor radius effects through full-orbit simulations

Need to perform simulations in full-orbit, following [Martinell PoP 2025]

↪ Energies characteristic of NBI heating (10 keV and 50 keV)

↪ Similar behaviour due to island rotation (resonances effect)

↪ But GC less sensitive to magnetic islands than FO

In TAPAS, full-orbit seems to produce less transport than GC (α particles at 3.5 MeV with an island width $\sim\rho_\alpha$)

Transport remains non-diffusive

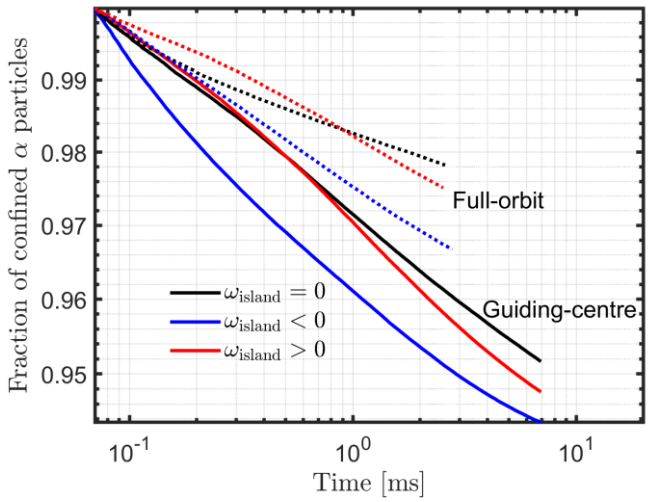

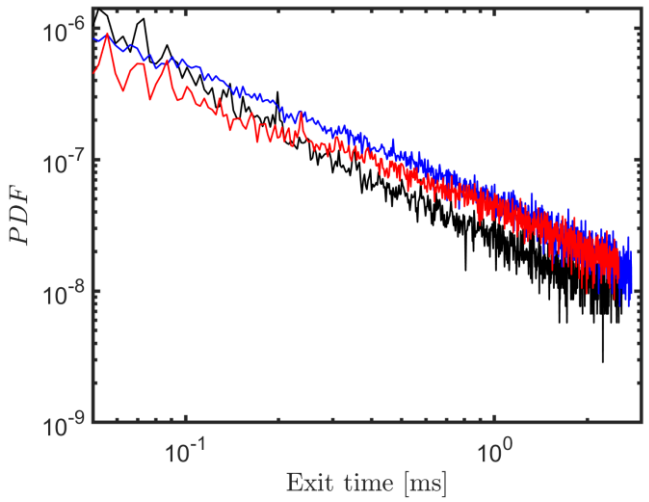

Finite Larmor radius effects through full-orbit simulations

Need to perform simulations in full-orbit, following [Martinell PoP 2025]

↪ Energies characteristic of NBI heating (10 keV and 50 keV)

↪ Similar behaviour due to island rotation (resonances effect)

↪ But GC less sensitive to magnetic islands than FO

In TAPAS, full-orbit seems to produce less transport than GC (α particles at 3.5 MeV with an island width $\sim\rho_\alpha$)

Transport remains non-diffusive

Analyse JET discharges using either an equivalent Maxwellian or during the slowing-down process with an α particle source (ongoing work with J. Varela and J. Garcia)

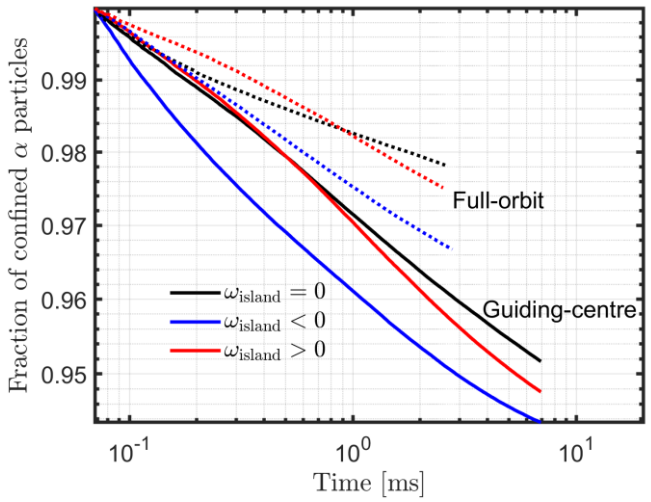

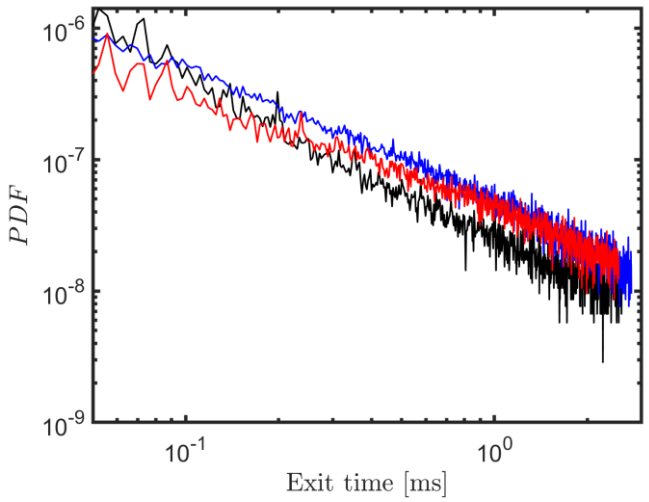

Outline of the presentation

Fundamental physics of energetic particles in tokamaks and basics on transport

Toroidal Accelerated PArticle Simulator (TAPAS)

↪ Example of application to realistic experimental case

Non axi-symmetric modes, both static and rotating (tearing modes)

↪ Purely magnetic large scale $(m, n) = (2,1)$, $\omega \ll 0$

Ion-temperature gradient (ITG) driven turbulence

↪ Electrostatic with a broad spectrum (m, n, k_r)

Absence of turbulence-induced EP transport in experiments

- **TFTR**: passing MeV fusion products exhibited $D_{EP} \approx 0.1 m^2/s$, smaller than thermal diffusivity [Zweben NF1991], especially in DT plasmas [Zweben NF1995] unlikely due to plasma fluctuations [Zweben PoP1994], but mainly to ripple effects [Yavorskij NF1998]. For beam EP, there is no clear conclusion [Ruskov NF1995, Ruskov PRL1995]. No significant EP anomalous transport and losses were observed in TFTR.

- Similar results for **JT-60U** (EP transport in reversed shear operations due to ripple effects [Tobita Nucl. Fusion 1997]) and **JET** (agreeement between modelling and experiments by setting $D_{EP} \ll D_{th}$ [Baranov PPCF2009]). No significant EP anomalous transport and losses were observed in JT-60U and JET.

- Similar results for on-axis NBI in **DIII-D** [Pace NF 2011]. EP transport induced by turbulence is too small to be experimentally relevant [Pace PoP2013]

Evidence of turbulence-induced EP transport in experiments

- **AUG**: for realistic experimental conditions, $D_{EP} \sim D_{th}$ and the experimental results indicate a redistribution of EP driven by turbulent [Günter NF2007]
- **DIII-D**: off-axis NBCD gave a peak of $D_{EP} \sim 1m^2/s$ for $E_b = 40$ keV, decreasing with E_b/T (transport beyond $E/T \gg 10$ is negligible and turbulence affects equally passing and trapped ions [Heidbrink PRL 2009]).
- **TORPEX (SMT)**: Suprathermal ion turbulent transport is nondiffusive, ranging from subdiffusive $\longrightarrow$ superdiffusive depending on the interplay of turbulent structures and ion orbits [Gustafson PRL 2012, Bovet PRL 2014, Furno PPCF 2015]

Turbulence-induced EP transport in simulations and theory

- **Electrostatic simulations with GYRO**: turbulence-induced α transport exhibits significant values for typical parameters in ITER, due to the curvature drift [Estrada-Mila PoP2006]
- **Electrostatic simulations with GKW**: the α particles are transported only for small values of E/T, no EP transport occurs above the slowing down critical energy [Angioni PoP 2008].
- **Electrostatic simulations with GTC**: diffusivity decreases drastically at high particle energy w.r.t. plasma temperature due to gyro-averaging effects and the probability density function of the ion radial excursion is found to be very close to a Gaussian, indicating a diffusive transport process [Zhang PRL 2008, Zhang PoP 2010, Zhang PRL 2011]. $D_{EP,passing} \sim E^{-1}$ and $D_{EP,trapped} \sim E^{-2}$, based on quasi-linear diffusion calculations including the resonance $\omega_{turb} - n_2\Omega_2 - n_3\Omega_3$.

Turbulence-induced EP transport in simulations and theory

- **Electromagnetic simulations with GENE**: orbit average is not valid under generic conditions and perpendicular decorrelation leads to E^{-1} decay of electrostatic diffusivity. Separating electrostatic from magnetic seems to be important, since the magnetic diffusivity is independent of E [Hauff PRL 2009, Jenko PRL 2011]. $D_{EP,passing} \sim E^{-1}$ and $D_{EP,trapped} \sim E^{-3/2}$
- **Quasi-linear modelling with TGLF, DEP and NUBEAM**: transport of EP due to coherent fluctuations is considerably larger than that due to micro-turbulence [Pace PoP 2013]
- **Semi-analytical approach** based on the decorrelation trajectory method: fusion-born α particle transport is expected only at $E \sim 100$ keV [Croitoru NF 2017]
- **Direct numerical simulation** using a given spectrum: nonlinear coupling between turbulence and RMPs enhances radial diffusion [Palade PoP 2021]

Examples of some scalings reported in gyrokinetics

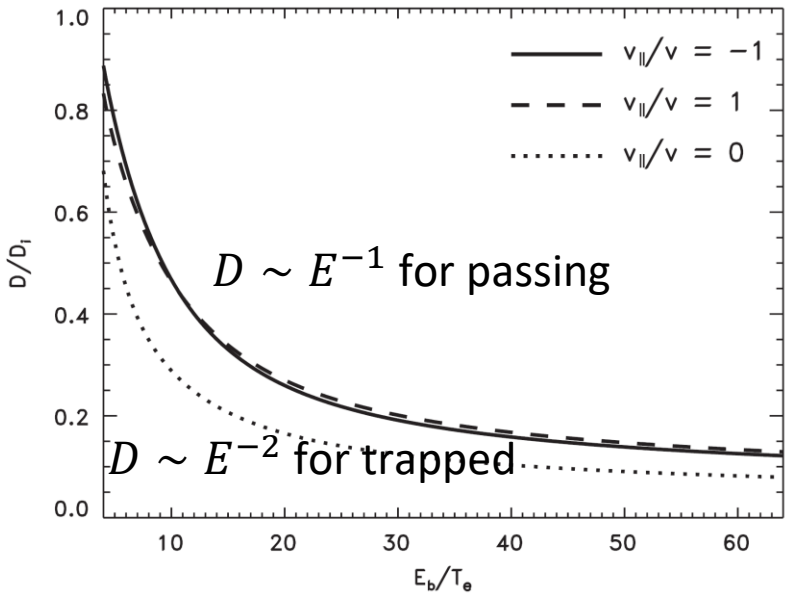

[From Zhang et al PRL 2008]

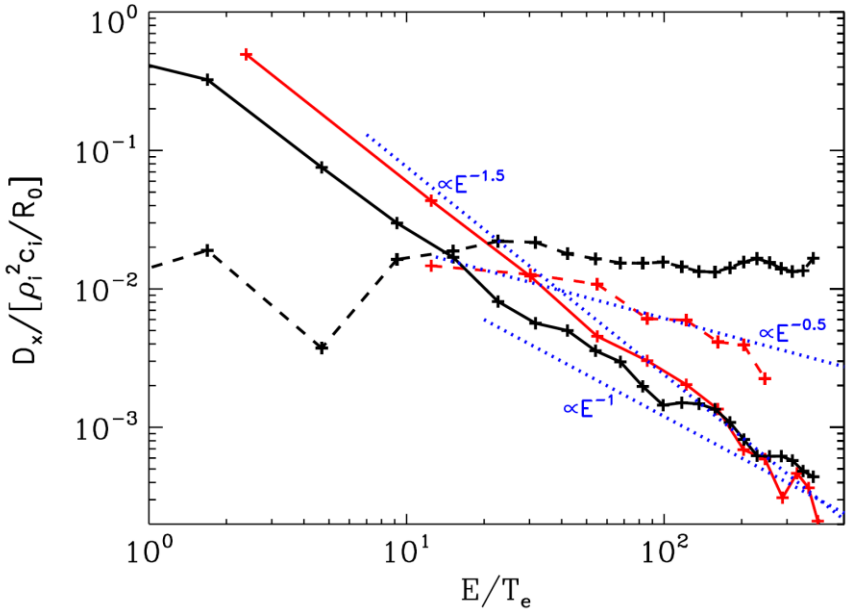

[From Hauff et al PRL 2009]

Ion Temperature Gradient driven turbulence

GYSELA [Grandgirard CPC 2016] solves the full-F gyro-kinetic equation in flux-driven and gradient-driven configurations, with collisions, coupled to the quasi-neutrality equation and Ampère's law.

We use here a standard electrostatic ITG simulation with adiabatic electrons, flux-driven (source), collisions, parabolic q-profile from 1.1 to 4.5, $R/L_T = 9, R/L_n = 2.5$ and buffer regions in the outer boundary

Reference values are $T_{ref} = 5$ keV, $B_{ref} = 3$ T, $R_0 = 3$ m, $m_{ref} = 2m_p$, $Z_{ref} = 1$.

Initialize mono-energetic α particles inside the turbulent region with $25 < E_\alpha/T < 600$, with Δt required to get good conservation properties for $E/T = 600$ (check that $\Delta E = -\int dt\, eZ\boldsymbol{v} \cdot \boldsymbol{\nabla}\phi$)

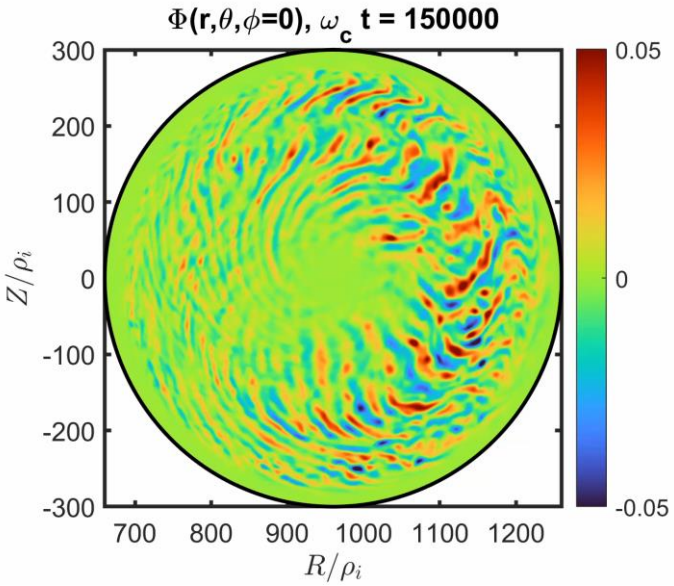

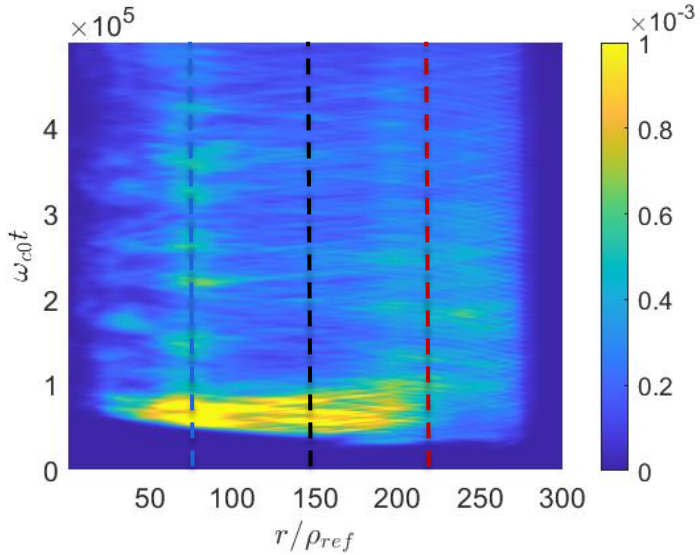

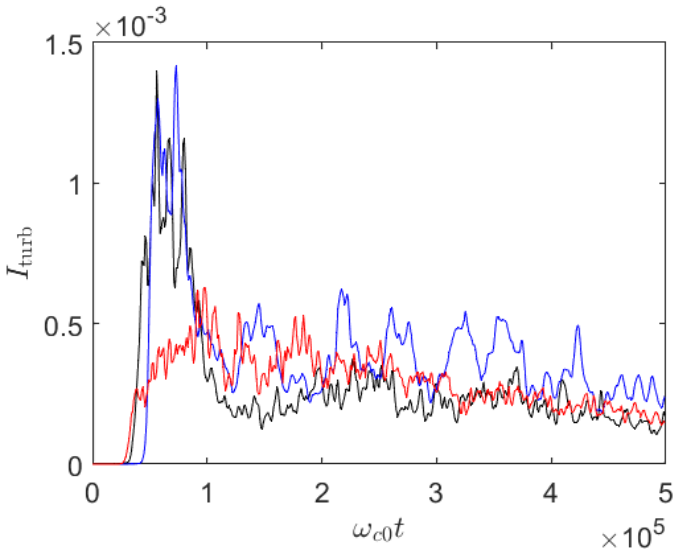

Energy diffusion coefficient decreases with E/T

No α particle losses for deeply passing/trapped below $E_\alpha/T = 100$. Losses of 1-2% peaked at $E_\alpha/T \approx 250$ (trapped) and $E_\alpha/T \approx 300$ (passing). Difference likely due to the orbit widths of trapped/passing.

The effect on the kinetic energy of particles remains small. The diffusivity decreases with E_α/T.

$\omega_{turb} - n_2\Omega_2 - n_3\Omega_3 \approx 0 \Rightarrow n_2\Omega_2 + n_3\Omega_3 \approx 0$, especially for high energies $\longrightarrow$ Changes in the kinetic energy are small

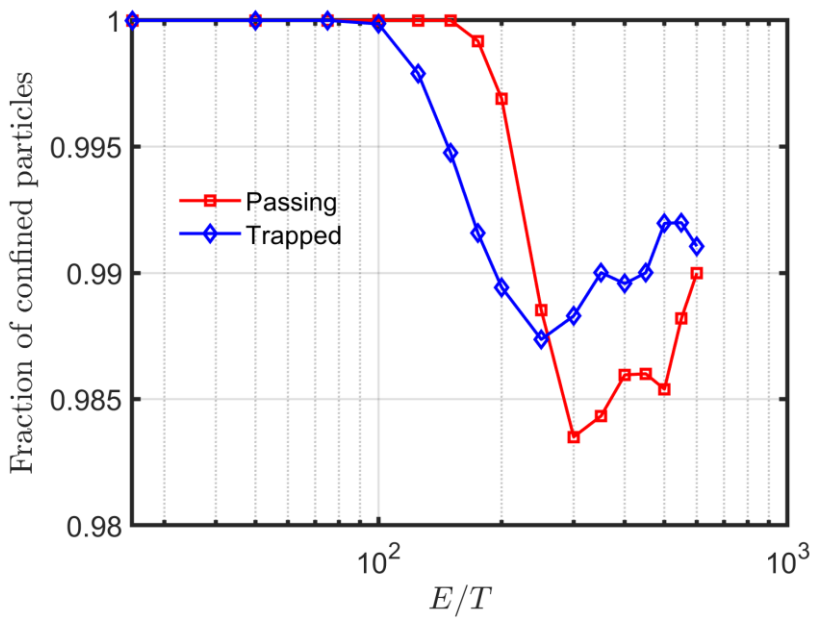

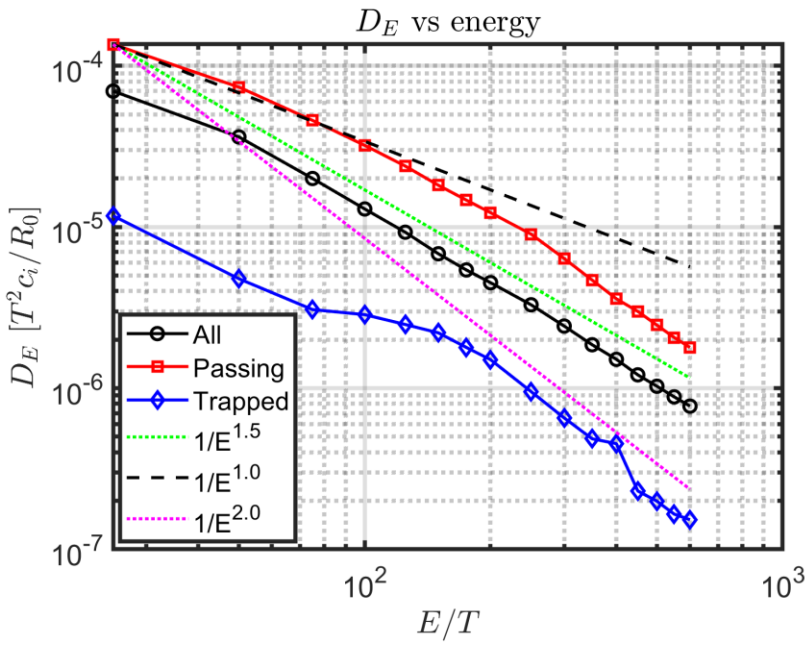

Non trivial behaviour of the radial dynamics

Considering all the particles, the diffusivity decreases with the energy as $D_r \sim 1/E^{\alpha}$, with $1 < \alpha < 3/2$.
Significant differences appear when classifying the particles in passing and trapped.

↪ The scaling is $D_r \sim E^{-\frac{3}{2}}$ for small energies ($E < 100T$ for trapped and $E < 200T$ for passing).
↪ Beyond those energies, the diffusivity exhibits a local maximum
Same behaviour for the mean radial velocity

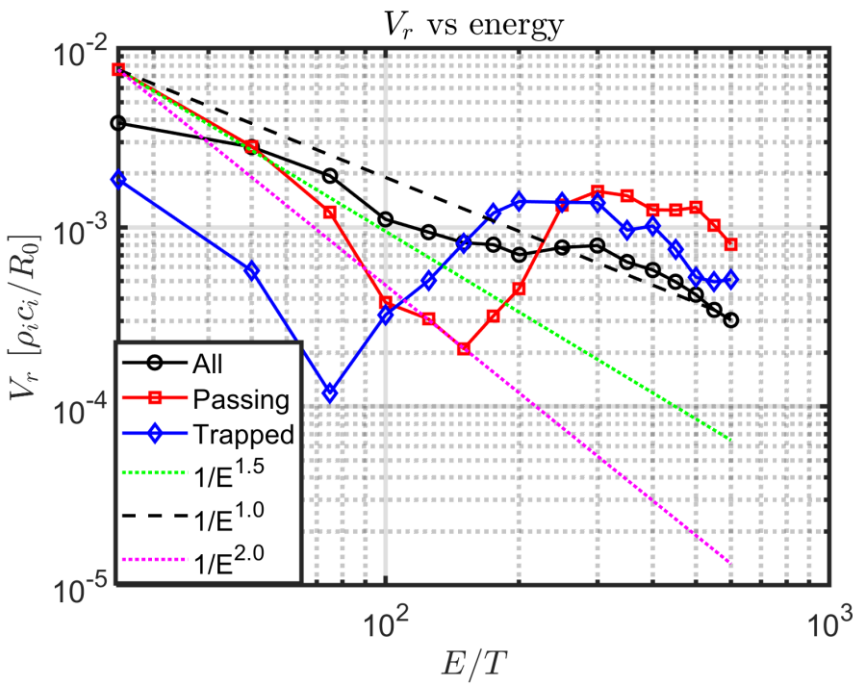

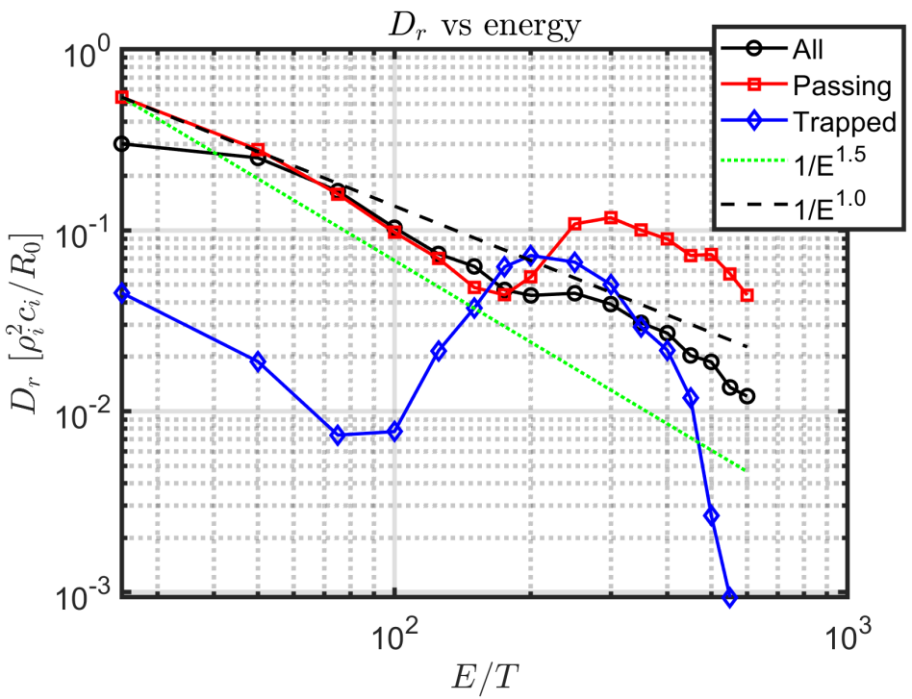

Non trivial behaviour of the radial dynamics

Considering all the particles, the diffusivity decreases with the energy as $D_r \sim 1/E^{\alpha}$, with $1 < \alpha < 3/2$.
Significant differences appear when classifying the particles in passing and trapped.

↪ The scaling is $D_r \sim E^{-\frac{3}{2}}$ for small energies ($E < 100T$ for trapped and $E < 200T$ for passing).
↪ Beyond those energies, the diffusivity exhibits a local maximum
Same behaviour for the mean radial velocity
Guiding-centre calculations give increased transport, similar behaviour for the diffusion coefficient, inverted behaviour for trapped-passing particles in terms of mean radial displacement

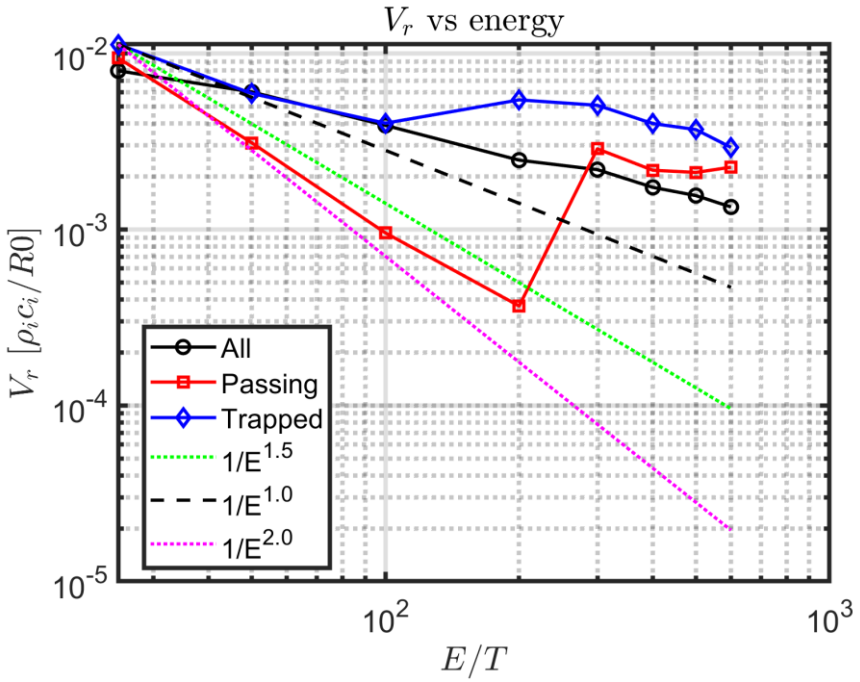

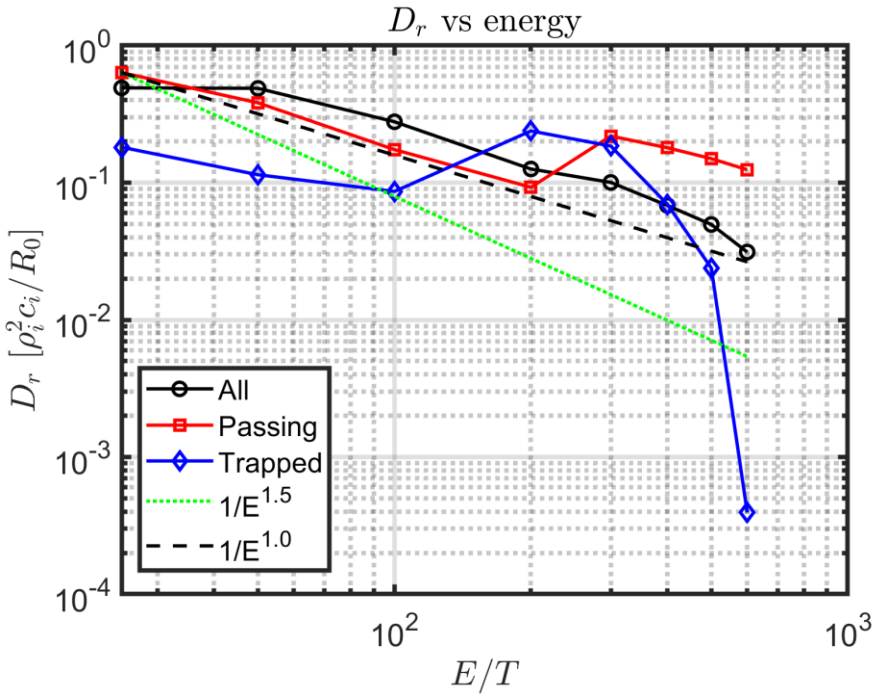

Non trivial behaviour of the radial dynamics

Considering all the particles, the diffusivity decreases with the energy as $D_r \sim 1/E^{\alpha}$, with $1 < \alpha < 3/2$.
Significant differences appear when classifying the particles in passing and trapped.

↪ The scaling is $D_r \sim E^{-\frac{3}{2}}$ for small energies ($E < 100T$ for trapped and $E < 200T$ for passing).
↪ Beyond those energies, the diffusivity exhibits a local maximum
Same behaviour for the mean radial velocity
Guiding-centre calculations give increased transport, similar behaviour for the diffusion coefficient, inverted behaviour for trapped-passing particles in terms of mean radial displacement

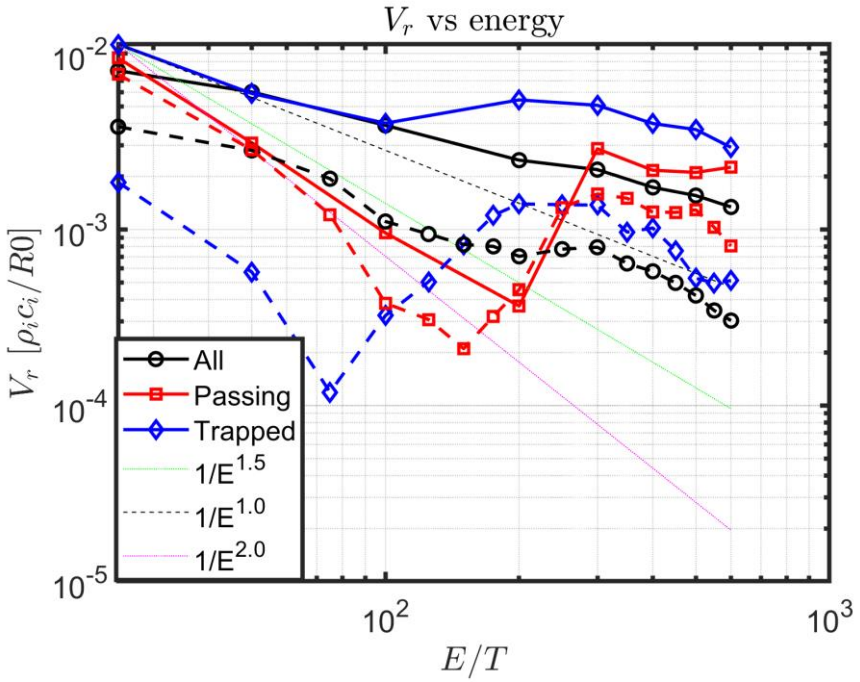

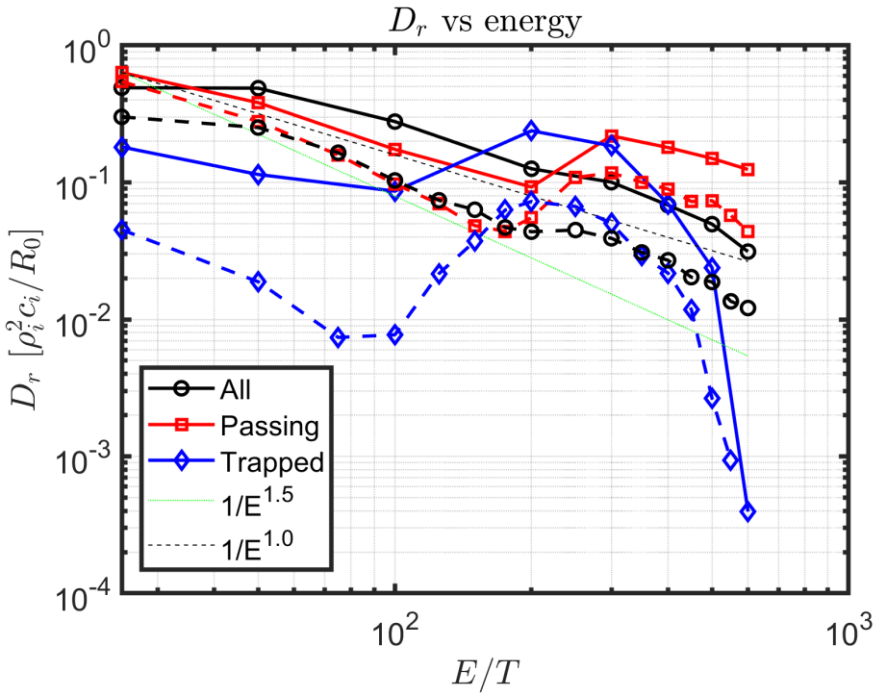

Possible reasons for the observed scaling

- Particles with $\lambda < -0.6$ (counter-passing) and $-0.3 < \lambda < 0$ (trapped close to the prompt losses region) are lost.
- The energy remains almost constant $\omega - n_2\Omega_2 - n_3\Omega_3 \approx n_2\Omega_2 + n_3\Omega_3 = 0$

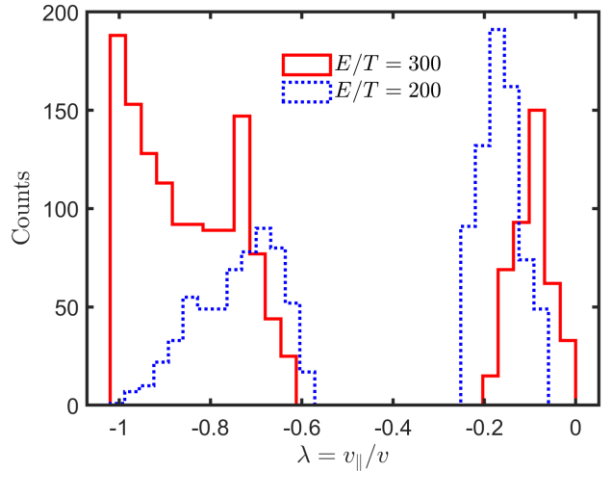

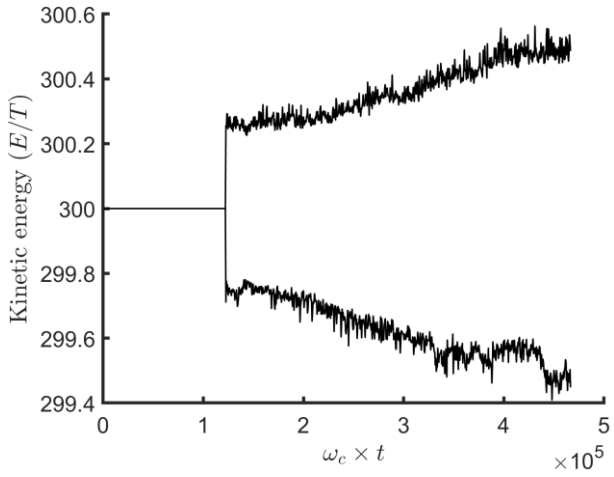

Possible reasons for the observed scaling

- Particles with $\lambda < -0.6$ (counter-passing) and $-0.3 < \lambda < 0$ (trapped close to the prompt losses region) are lost.
- The energy remains almost constant $\omega - n_2\Omega_2 - n_3\Omega_3 \approx n_2\Omega_2 + n_3\Omega_3 = 0$

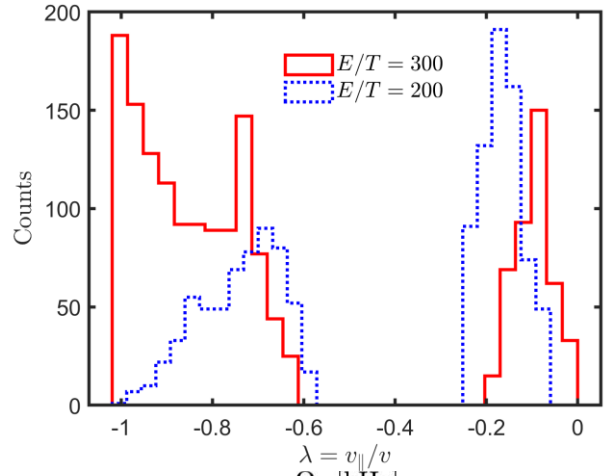

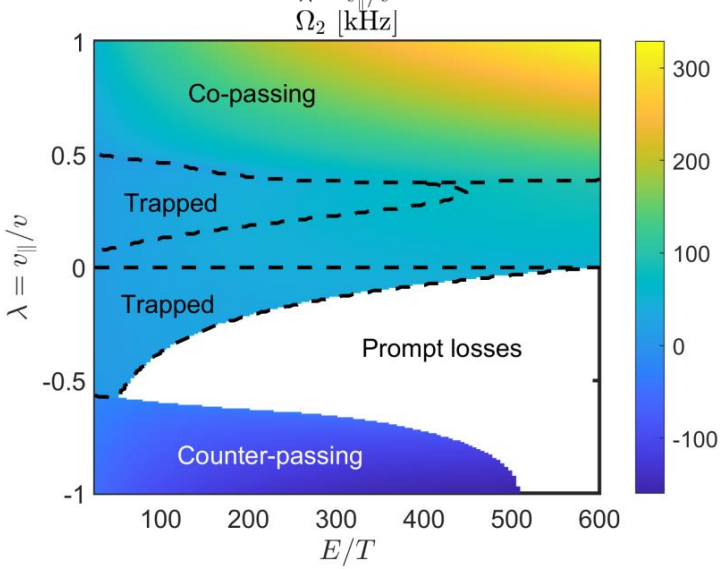

Possible reasons for the observed scaling

- Particles with $\lambda < -0.6$ (counter-passing) and $-0.3 < \lambda < 0$ (trapped close to the prompt losses region) are lost.
- The energy remains almost constant $\omega - n_2\Omega_2 - n_3\Omega_3 \approx n_2\Omega_2 + n_3\Omega_3 = 0$
  - Presence of resonances for the turbulent modes that can lead to the observed losses.

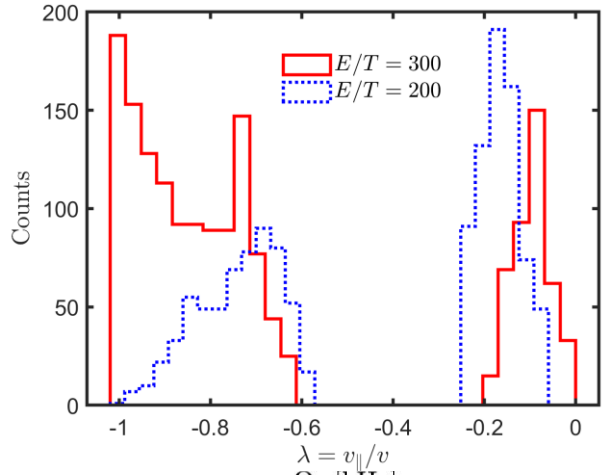

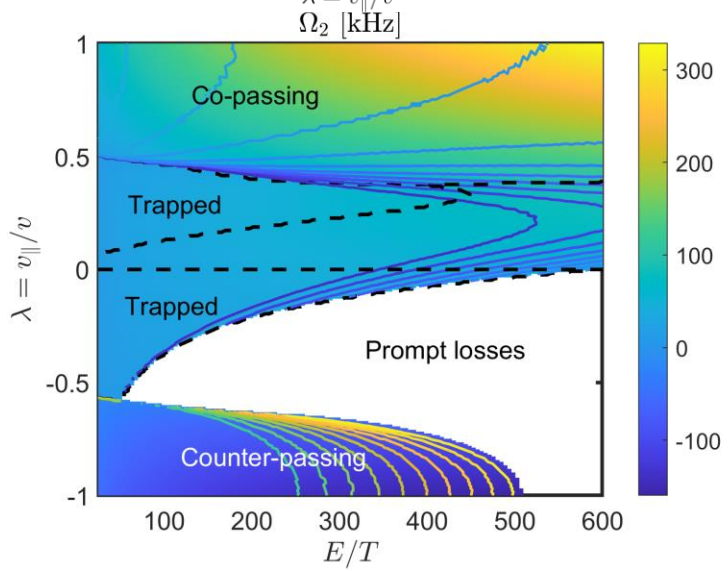

Possible reasons for the observed scaling

- Particles with $\lambda < -0.6$ (counter-passing) and $-0.3 < \lambda < 0$ (trapped close to the prompt losses region) are lost.
- The energy remains almost constant $\omega - n_2\Omega_2 - n_3\Omega_3 \approx n_2\Omega_2 + n_3\Omega_3 = 0$
  - Presence of resonances for the turbulent modes that can lead to the observed losses.
- Further analyses are required to assess the diffusive nature of the transport
  - For small energies, the PDF of displacements exhibits a Gaussian behaviour
  - For larger energies, the PDF departs from a Gaussian
  - Superdiffusion occurs when turbulent structures are relatively static with respect to the ions beyond a given threshold in turbulence amplitude [Gustafson PRL 2012]

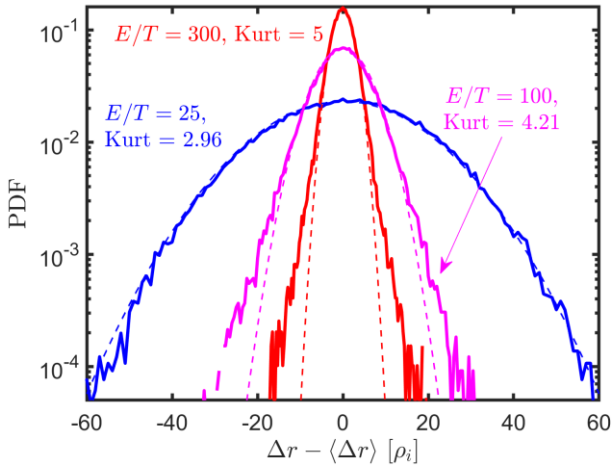

Future directions

- Radial dependence of D_r
- Different regimes of turbulence (amplitude, size of the machine)
- Different regimes of heating
  - α particle heating: analyses for a distribution function (instead of mono-energetic simulations) and during the slowing-down process
  - NBI (and ICRH): use the ionization (and RF) module of TAPAS in realistic configurations together with the collision operator
- Perform longer simulations
  - With a 3D non evolving potential ($\omega_{turbulence} \ll \Omega_2, \Omega_3$ for high energies).
  - With synthetic turbulence using generative deep-learning [Clavier PRE 2025, Clavier PoP 2025, Liu PhysRevFluids 2025] (see poster by B. Clavier)

Summary

- Complexity of the dynamics of energetic particles
- Use of the Toroidal Accelerated Particle Simulator (TAPAS) to study EP transport phenomena (used for DIII-D RSAE case)
- Analyses of different cases show a non-diffusive behaviour of EP transport
  - Short times and radial scales $\longrightarrow$ Nondiffusive $\approx$ Diffusive
  - Need to extent the models for long time regimes involving several spatial scales
- Further studies are required to assess the diffusive/no-difffusive transport depending on the regimes

BACK-UP SLIDES

amU
Aix Marseille Université

Motion invariants to characterise EP trajectories

We define an equilibrium Hamiltonian $H_{eq}(\boldsymbol{J}) = \int d\boldsymbol{\alpha} H(\boldsymbol{\alpha}, \boldsymbol{J})$

$\Rightarrow \boldsymbol{J}$ are motion invariants associated to the three periodic directions

$$J_1 = -\frac{m\mu}{eZ} \qquad J_2 = \Phi(J_3) + \frac{1}{2\pi}\int_0^{2\pi} m\boldsymbol{v}\cdot\boldsymbol{b}ds \qquad J_3 \equiv P_\varphi = -eZ\psi + m\frac{B_\varphi}{B}v_\parallel$$

$$\Omega_1 = \frac{\partial H_{eq}}{\partial J_1} \qquad \Omega_2 = \frac{\partial H_{eq}}{\partial J_2} \qquad \Omega_3 = \frac{\partial H_{eq}}{\partial J_3}$$

Motion invariants to characterise EP trajectories

We define an equilibrium Hamiltonian $H_{eq}(\boldsymbol{J}) = \int d\boldsymbol{\alpha} H(\boldsymbol{\alpha}, \boldsymbol{J})$

$\Rightarrow \boldsymbol{J}$ are motion invariants associated to the three periodic directions

$$\Omega_1 = \frac{\partial H_{eq}}{\partial J_1}$$

$$\Omega_2 = \frac{\partial H_{eq}}{\partial J_2}$$

$$\Omega_3 = \frac{\partial H_{eq}}{\partial J_3}$$

Motion invariants to characterise EP trajectories

We define an equilibrium Hamiltonian $H_{eq}(\boldsymbol{J}) = \int d\boldsymbol{\alpha} H(\boldsymbol{\alpha}, \boldsymbol{J})$

$\Rightarrow \boldsymbol{J}$ are motion invariants associated to the three periodic directions

$$\Omega_1 = \frac{\partial H_{eq}}{\partial J_1} \Rightarrow \Omega_1 = \frac{eZB}{m}$$

$$\Omega_2 = \frac{\partial H_{eq}}{\partial J_2} \Rightarrow \Omega_2 = \Omega_{c,th}\rho_\star \epsilon_a \sigma \frac{1}{q}\sqrt{E - (1-\epsilon)\mu B_0}\frac{\pi}{\sqrt{2}}\begin{cases} \mathbb{K}^{-1}(\kappa), \kappa < 1 \\ \kappa \mathbb{K}^{-1}\left(\frac{1}{\kappa}\right), \kappa > 1 \end{cases}$$

$$\Omega_3 = \frac{\partial H_{eq}}{\partial J_3} \Rightarrow \Omega_3 = \Omega_{c,th}\rho_\star \epsilon_a \frac{\Omega_t}{\Omega_{c,th}}\frac{qE}{\epsilon}\overline{\Omega}_d + \delta_{passing} q \Omega_2$$

[Zarzoso PoP2019]

Motion invariants to characterise EP trajectories

We define an equilibrium Hamiltonian $H_{eq}(\boldsymbol{J}) = \int d\boldsymbol{\alpha} H(\boldsymbol{\alpha}, \boldsymbol{J})$

$\Rightarrow \boldsymbol{J}$ are motion invariants associated to the three periodic directions

$$\Omega_1 = \frac{\partial H_{eq}}{\partial J_1} \Rightarrow \Omega_1 = \frac{eZB}{m}$$

$$\Omega_2 = \frac{\partial H_{eq}}{\partial J_2} \Rightarrow \Omega_{2,passing} \approx \frac{v_\parallel}{qR_0}, \Omega_{2,trapped} \approx \frac{v}{qR_0}\sqrt{\frac{\epsilon}{2}}$$

$$\Omega_3 = \frac{\partial H_{eq}}{\partial J_3} \Rightarrow \Omega_{3,passing} = \frac{v_\parallel}{R_0}, \Omega_{3,trapped} \approx \frac{qE}{eZB_0R_0r}$$

E_α =	500 keV	1 MeV	3,5 MeV
$\Omega_{2,passing}$	130 kHz	180 kHz	340 kHz
$\Omega_{3,passing}$	260 kHz	360 kHz	680 kHz
$\Omega_{2,trapped}$	50 kHz	70 kHz	130 kHz
$\Omega_{3,trapped}$	10 kHz	20 kHz	60 kHz

Fundamental and high order resonances

If $\Omega_1 \gg \omega \Rightarrow n_1 = 0 \Leftrightarrow \frac{1}{2\pi}\oint \mathrm{d}\varphi_c \Rightarrow$ Linear resonance: $\omega - n_2\Omega_2 - n_3\Omega_3 = 0$

Nonlinear resonances should also be considered if the amplitude of the perturbation is sufficiently large to strongly modify the unperturbed trajectories [Sanchis PPCF 2018]

$\theta = \delta_{passing}\alpha_2 + \theta_0\Theta(\alpha_2), \psi = \bar{\psi} + \hat{\psi}_0\Xi(\alpha_2)$ with Θ, Ξ periodic functions of α_2

↪ Deeply trapped particles $\Rightarrow \theta \approx \theta_0 \sin\alpha_2$

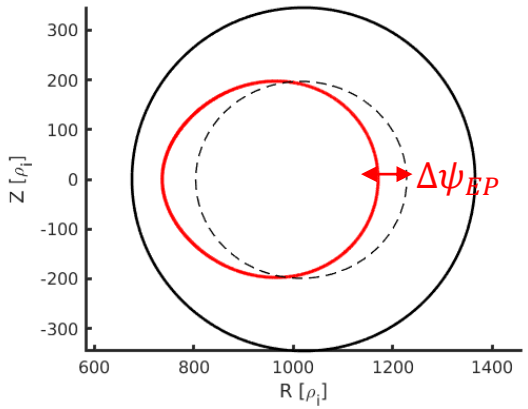

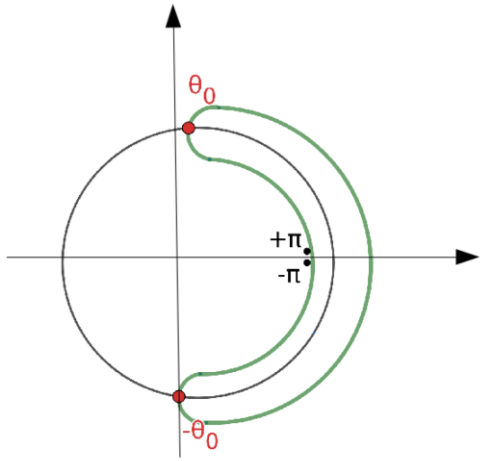

$$H = H_{m,n}(\psi)e^{i(m\theta+n\varphi)} = e^{\Xi(\alpha_2)\partial_\psi}H_{m,n}(\bar{\psi})e^{i(m\Theta(\alpha_2)+n\varphi)} = \sum_{n_2} \ldots J_{n_2}(\hat{\psi}_0 k_\psi)e^{in_2\alpha_2}$$

Fundamental and high order resonances

$$F = F_{\mathrm{eq}}(\mathbf{J}) + \sum_{\mathbf{n}\omega} \delta F_{\mathbf{n}\omega} e^{i(\mathbf{n}\cdot\boldsymbol{\alpha}-\omega t)}$$

$$H = H_{\mathrm{eq}}(\mathbf{J}) + \sum_{\mathbf{n}\omega} \delta H_{\mathbf{n}\omega} e^{i(\mathbf{n}\cdot\boldsymbol{\alpha}-\omega t)}$$

$$\Rightarrow \delta F_{\mathbf{n},\omega} = -\frac{\mathbf{n}\cdot\partial_{\mathbf{J}} F_{\mathrm{eq}}}{\omega - \mathbf{n}\cdot\Omega}\delta H_{\mathbf{n}\omega}$$

If $\Omega_1 \gg \omega \Rightarrow n_1 = 0 \Leftrightarrow \frac{1}{2\pi}\oint \mathrm{d}\varphi_c \Rightarrow$ Linear resonance: $\omega - n_2\Omega_2 - n_3\Omega_3 = 0$

Nonlinear resonances should also be considered if the amplitude of the perturbation is sufficiently large to strongly modify the unperturbed trajectories [Sanchis PPCF 2018]

$\theta = \delta_{passing}\alpha_2 + \theta_0\Theta(\alpha_2), \psi = \bar{\psi} + \hat{\psi}_0\Xi(\alpha_2)$ with Θ, Ξ periodic functions of α_2

↪ Deeply trapped particles $\Rightarrow \theta \approx \theta_0 \sin\alpha_2$

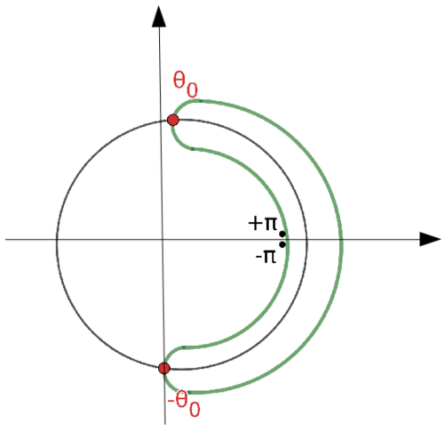

$$H = H_{m,n}(\psi)e^{i(m\theta+n\varphi)} = e^{\Xi(\alpha_2)\partial_\psi} H_{m,n}(\bar{\psi})e^{i(m\Theta(\alpha_2)+n\varphi)} = \sum_{n_2} \ldots J_{n_2}(\hat{\psi}_0 k_\psi)e^{in_2\alpha_2}$$

Computing the diffusion coefficient from microscopic displacements

Displacement in arbitrary direction: $\Delta x(t) = x(t) - x(0) \Rightarrow$ Lagrangian velocity: $v_x(t) = \frac{d\Delta x}{dt}$

Taylor's expression relates the Lagrangian velocity autocorrelation function to the rate of change of the variance of the displacement $\sigma_x^2 = \langle(\Delta x - \langle\Delta x\rangle)^2\rangle$

$$\frac{d\sigma_x^2}{dt} = 2\int_0^t \langle v_x(0)v_x(t')\rangle dt'$$

If the autocorrelation decays fast enough, $\lim_{t\to\infty} \int_0^t \langle v_x(0)v_x(t')\rangle dt'$ exists and the diffusion coefficient is

$$D = \lim_{t\to\infty} \int_0^t \langle v_x(0)v_x(t')\rangle dt' \Rightarrow \sigma_x^2 \sim t$$

In general $\sigma_x^2 \sim t^\gamma \begin{cases} \gamma < 1 \Rightarrow & \text{Subdiffusive} \\ \gamma = 1 \Rightarrow & \text{Diffusive} \\ 1 < \gamma < 2 \Rightarrow & \text{Superdiffusive} \\ \gamma = 2 \Rightarrow & \text{Ballistic} \end{cases}$

Collision operator in TAPAS

Collisions of energetic particles on a Maxwellian background, n_b, T_b, with electrons and ions

Essential for long time simulations, modelling the slowing-down of EP for alphas, NBI and ICRH

$$\mathrm{d}\mathbf{v}_{\text{coll, det}} = -\nu_s \mathrm{d}t\, \mathbf{v}$$

$$\mathrm{d}\mathbf{v}_{\text{coll, stoch}} = \left[\sqrt{D_\parallel}\frac{\mathbf{v}\otimes\mathbf{v}}{v^2} + \sqrt{D_\perp}\left(\mathbf{I} - \frac{\mathbf{v}\otimes\mathbf{v}}{v^2}\right)\right]\cdot \mathrm{d}\mathbf{W}^{\mathbf{v}}$$

$$\nu_s = \sum_b 4 n_b C_b \left(\frac{m_b}{2k_B T_b}\right)^{3/2} \frac{\psi(x)}{x}$$

$$D_\parallel = \sum_b 4 n_b C_b \left(\frac{m_b}{2k_B T_b}\right)^{1/2} \frac{\psi(x)}{x}$$

$$D_\perp = \sum_b 2 n_b C_b \left(\frac{m_b}{2k_B T_b}\right)^{1/2} \frac{\Phi(x) - \psi(x)}{x}$$

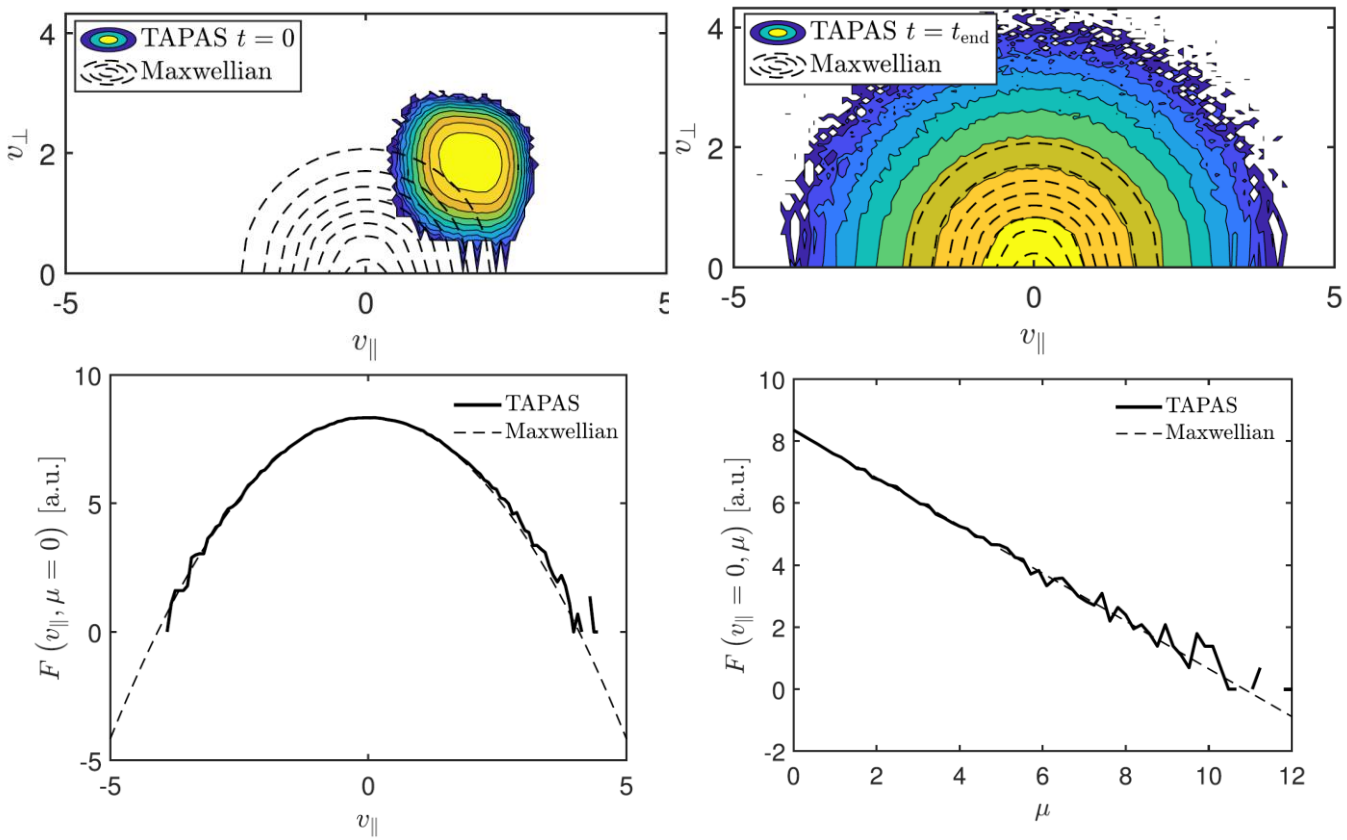

[H. Betar, D. Zarzoso *et al Nuclear Fusion* 2024]

Larmor radius of α particles

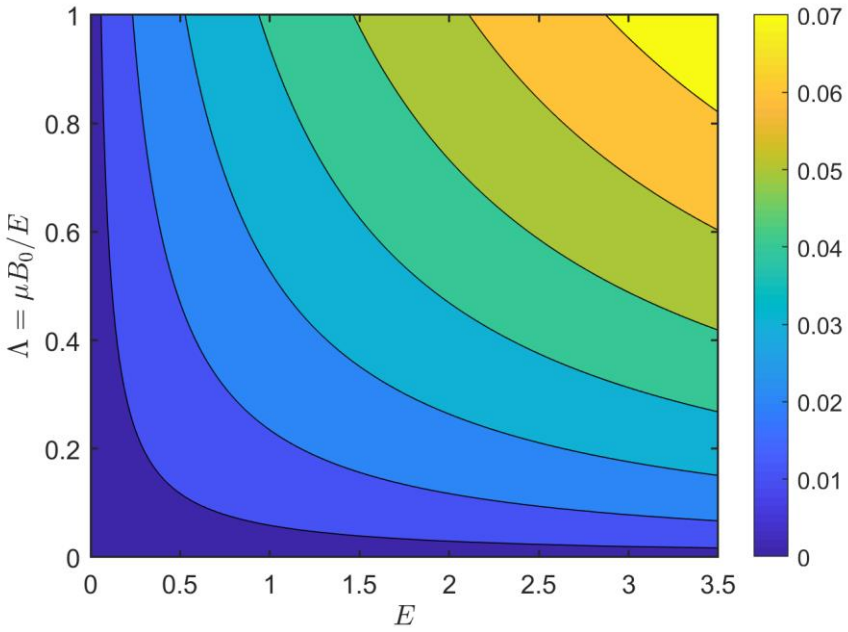

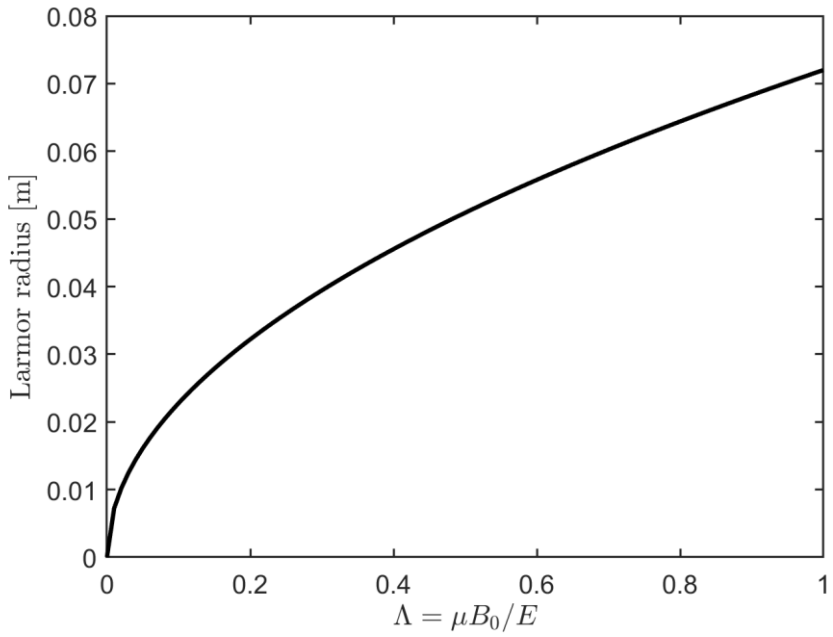

Some examples of EP transport reviewed in this presentation

Axi-symmetric modes or oscillating radial electric field (EGAM)

↪ Electrostatic large scale $(m, n) = (0,0)$, $\omega \approx \omega_{GAM} \neq 0$

Non axi-symmetric modes, both static and rotating (tearing modes)

↪ Purely magnetic large scale $(m, n) = (2,1)$, $\omega \ll 0$

Ion-temprature gradient (ITG) driven turbulence

↪ Electrostatic with a broad spectrum (m, n, k_r)

Oscillating $E_r \longrightarrow$ Anomalous transport and losses

Reduced model for the potential $\phi = [\phi_{00}(r) + \phi_{10}(r)\sin\theta]\cos\omega t$

> Oscillating radial electric field
>
> $\boldsymbol{v}_{E\times B} \cdot \boldsymbol{\nabla r} = 0 \Longrightarrow$ No convective transport

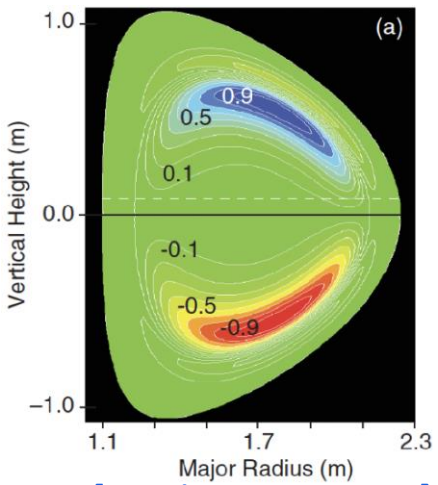

[Nazikian PRL 2008]

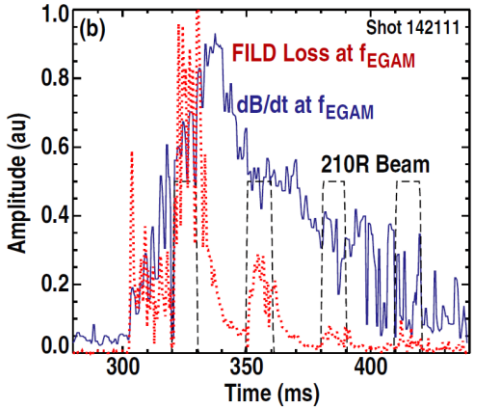

[Fisher NF 2012]

Oscillating $E_r \longrightarrow$ Anomalous transport and losses

Reduced model for the potential $\phi = [\phi_{00}(r) + \phi_{10}(r)\sin\theta]\cos\omega t$

- Oscillating radial electric field
- $\boldsymbol{v}_{E\times B} \cdot \boldsymbol{\nabla r} = 0 \Longrightarrow$ No convective transport

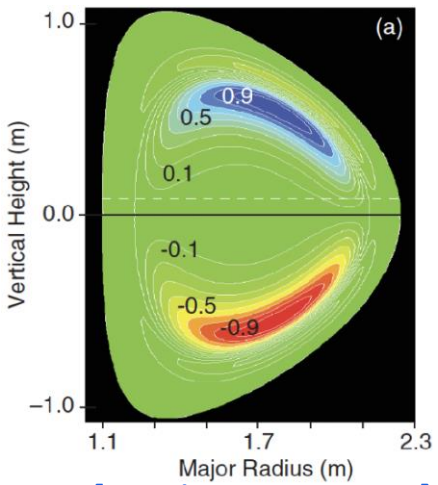

[Nazikian PRL 2008]

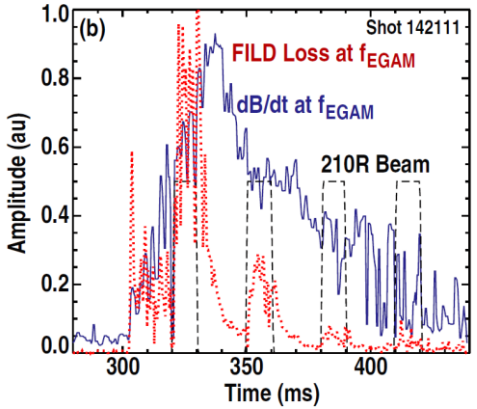

[Fisher NF 2012]

Oscillating $E_r \longrightarrow$ Anomalous transport and losses

Reduced model for the potential $\phi = [\phi_{00}(r) + \phi_{10}(r)\sin\theta]\cos\omega t$

Oscillating radial electric field

$\boldsymbol{v}_{E\times B} \cdot \boldsymbol{\nabla r} = 0 \Longrightarrow$ No convective transport

Analyse losses of energetic particles confined in the absence of perturbation, using the GC version of TAPAS

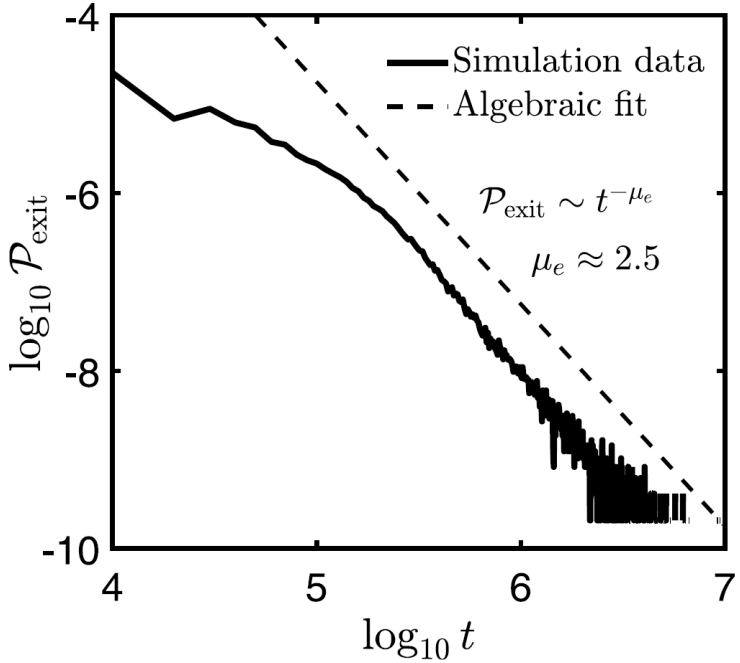

Algebraic decay of exit time

$\nparallel$

Exponential decay of exit time

$\Downarrow$

Radial transport is anomalous

Oscillating $E_r \longrightarrow$ Chaotic separatrix

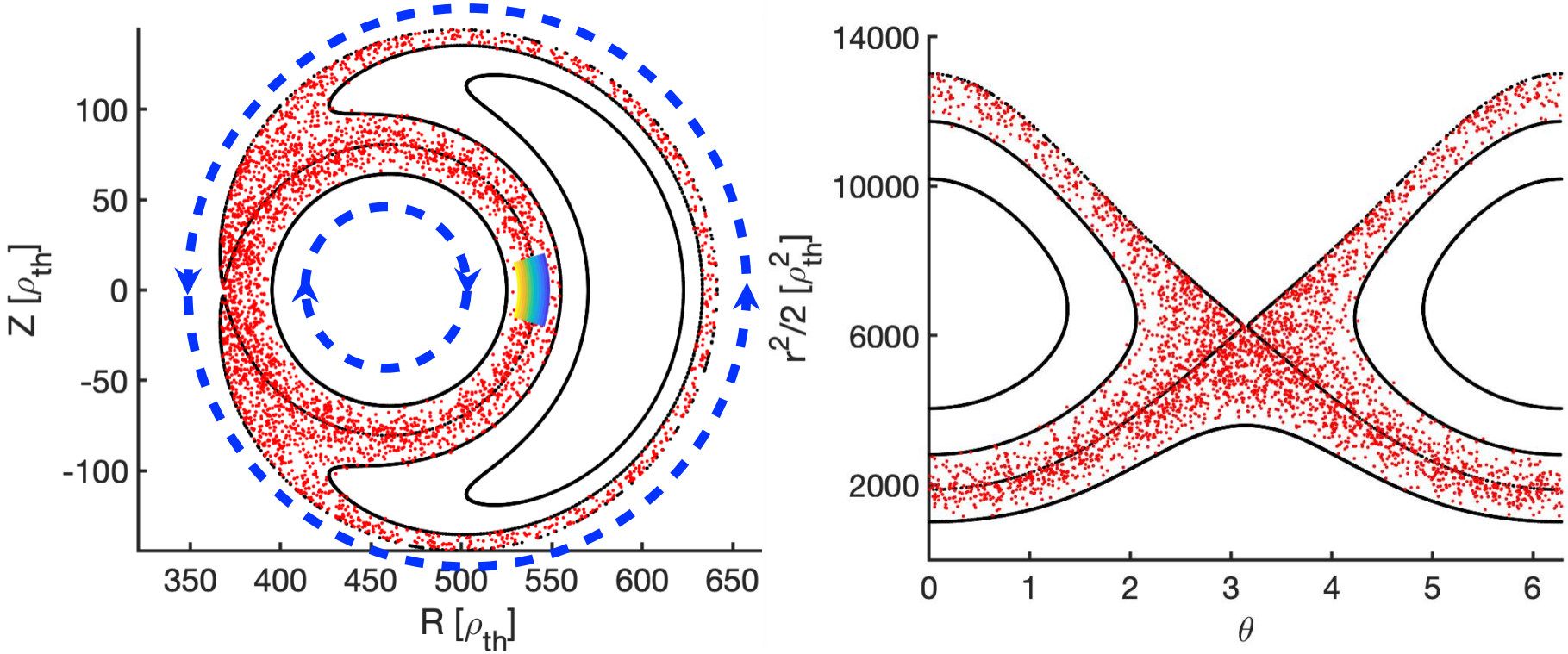

Without any perturbation → Integrable system. Trajectories = Passing & Trapped

Passing/Trapped boundary = separation between positive (co-passing) & negative (counter-passing) poloidal displacements

With perturbation → Chaotic separatrix: particles can alternate positive and negative displacements.

Transport of EP is non diffusive

Time-dependent variance

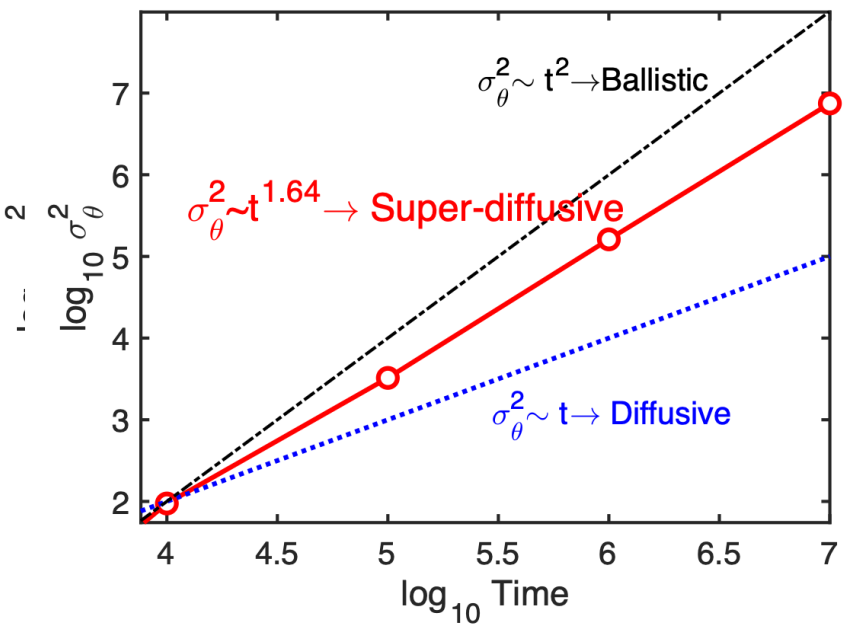

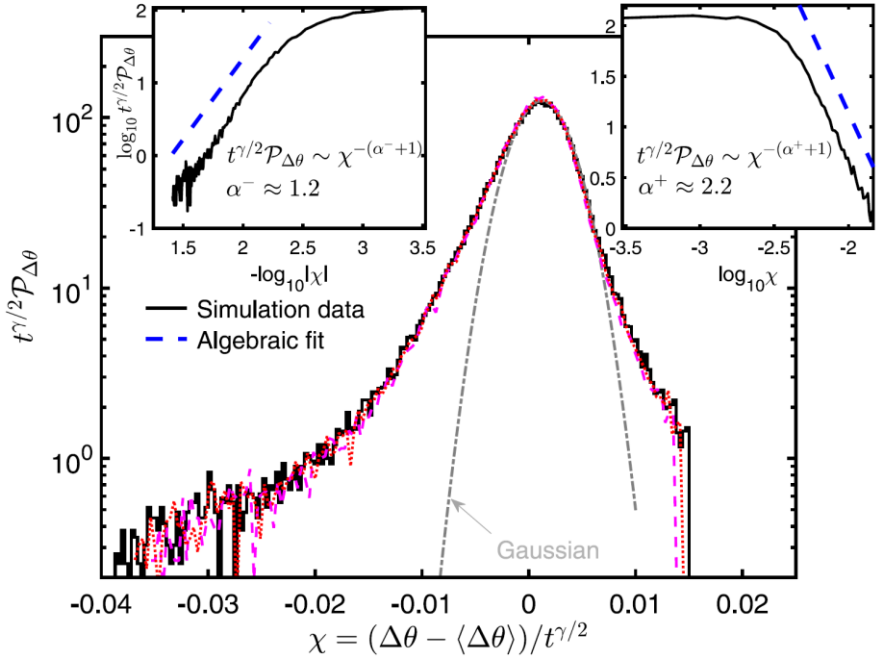

Poloidal spreading $\Delta\theta(t) = \theta(t) - \theta(t)$ observed when increasing time.

Study of the variance $\sigma_\theta^2 = \langle(\Delta\theta - \langle\Delta\theta\rangle)^2\rangle$

In our case: $\sigma_\theta^2 \sim t^\gamma$, with $\gamma = 1.64 \Rightarrow$ Super-diffusive transport (anomalous) transport

Reference Deuterium plasma for JET size (R_0=2.9m, a=1m, B_0=3.5T, T_{ref}=5keV)
Simplified circular geometry with concentric flux surfaces
Reversed q-profile from 1.5 to 7.0, tearing-unstable ($\Delta' > 0$)
$A_{\|}$ calculated from a shooting module

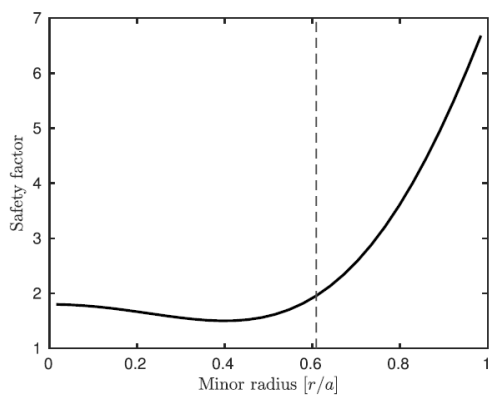

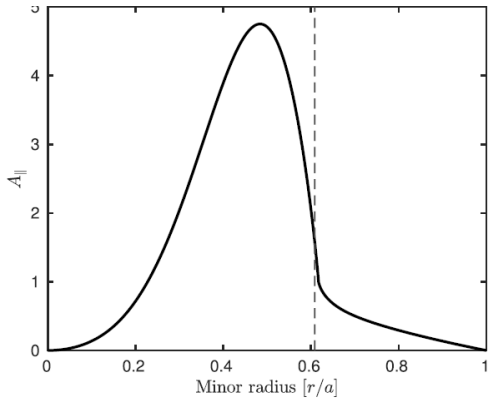

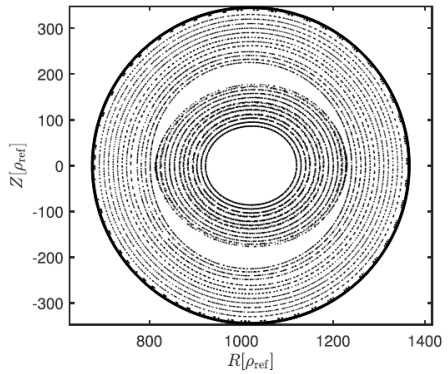

Exit probability

- Up-down symmetric
- Shifted following orbit drift w.r.t. flux surfaces
- Reflects the structure of the magnetic island

Mean exit time

- Same structure as the exit probability
- General behaviour: large exit times for low exit probability → rare events

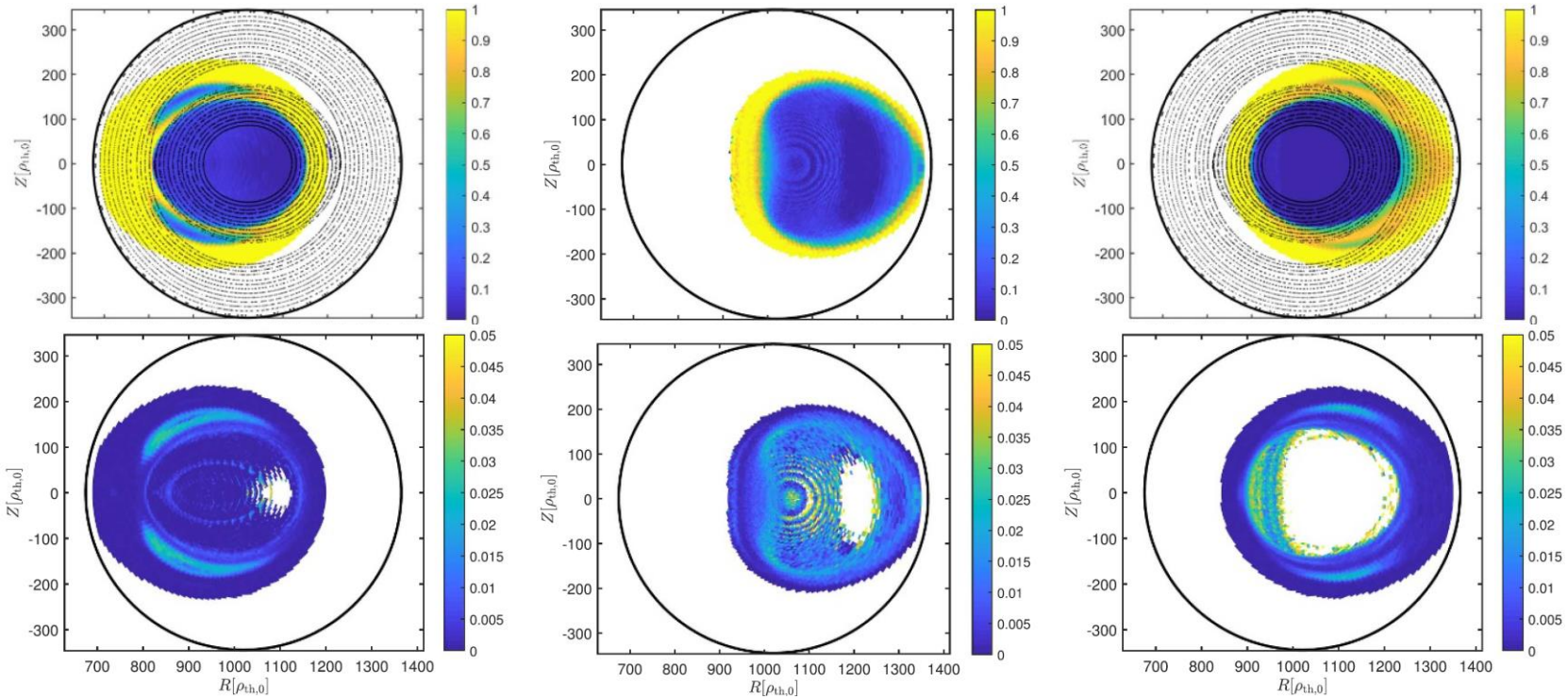

Methodology to compute the coefficients

Radial displacement $\Delta r = r - r(t = 0)$ for each particle

Mean radial displacement
$\langle \Delta r \rangle = \langle r - r(t = 0) \rangle$

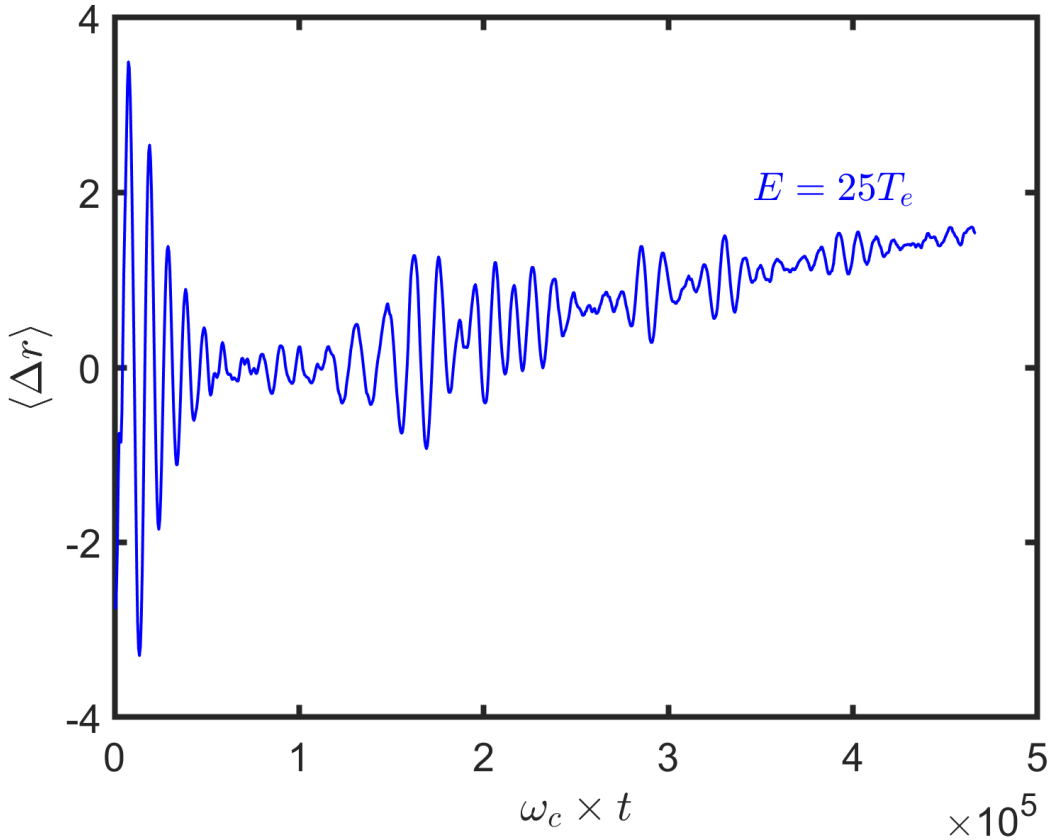

Methodology to compute the coefficients

Radial displacement $\Delta r = r - r(t = 0)$ for each particle

Mean radial displacement
$\langle \Delta r \rangle = \langle r - r(t = 0) \rangle$

Compute the « mean velocity» as $V_r = \frac{d\langle \Delta r \rangle}{dt}$

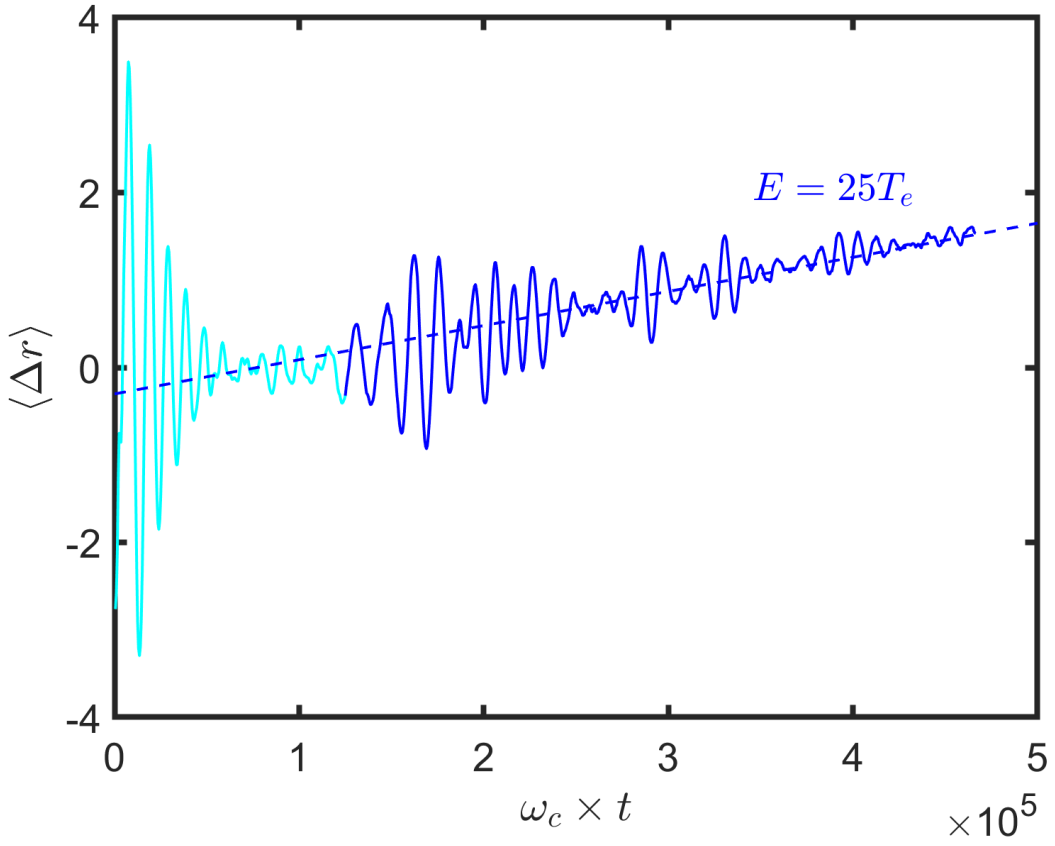

Methodology to compute the coefficients

Radial displacement $\Delta r = r - r(t = 0)$ for each particle

Mean radial displacement
$\langle \Delta r \rangle = \langle r - r(t = 0) \rangle$

Compute the « mean velocity» as $V_r = \frac{d\langle \Delta r \rangle}{dt}$

Variance $\sigma_r^2 = \langle (\Delta r - \langle \Delta r \rangle)^2 \rangle$

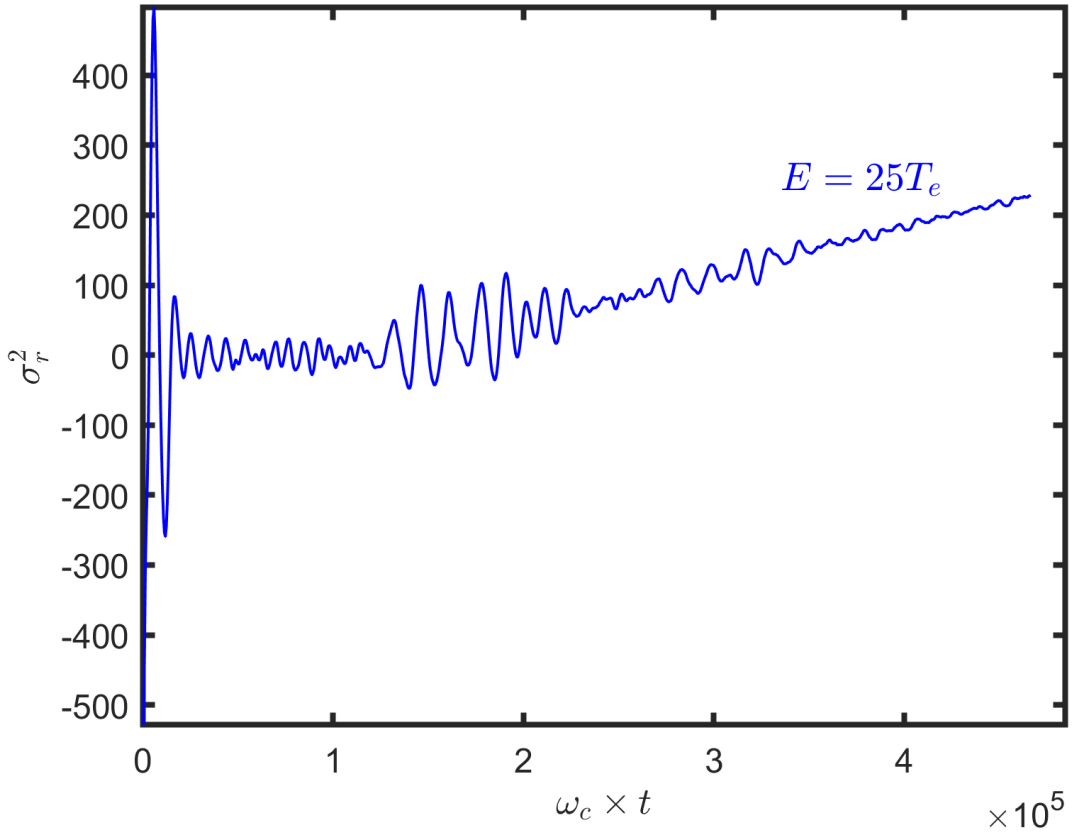

Methodology to compute the coefficients

Radial displacement $\Delta r = r - r(t = 0)$ for each particle

Mean radial displacement
$\langle \Delta r \rangle = \langle r - r(t = 0) \rangle$

Compute the « mean velocity» as $V_r = \frac{d\langle \Delta r \rangle}{dt}$

Variance $\sigma_r^2 = \langle (\Delta r - \langle \Delta r \rangle)^2 \rangle$

Compute the « diffusion coefficient » as $D_r = \frac{1}{2}\frac{d\sigma_r^2}{dt}$

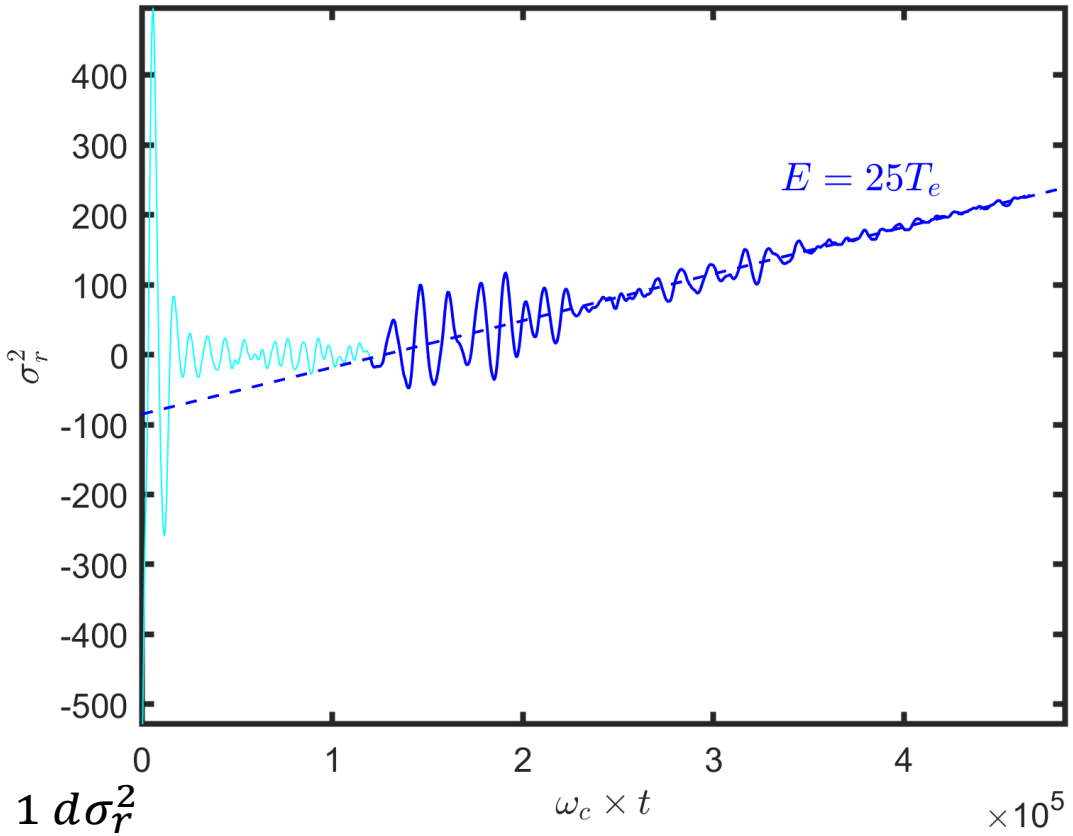

Methodology to compute the coefficients

Radial displacement $\Delta r = r - r(t = 0)$ for each particle

Mean radial displacement
$\langle \Delta r \rangle = \langle r - r(t = 0) \rangle$

Compute the « mean velocity» as $V_r = \frac{d\langle \Delta r \rangle}{dt}$

Variance $\sigma_r^2 = \langle (\Delta r - \langle \Delta r \rangle)^2 \rangle$

Compute the « diffusion coefficient » as $D_r = \frac{1}{2}\frac{d\sigma_r^2}{dt}$

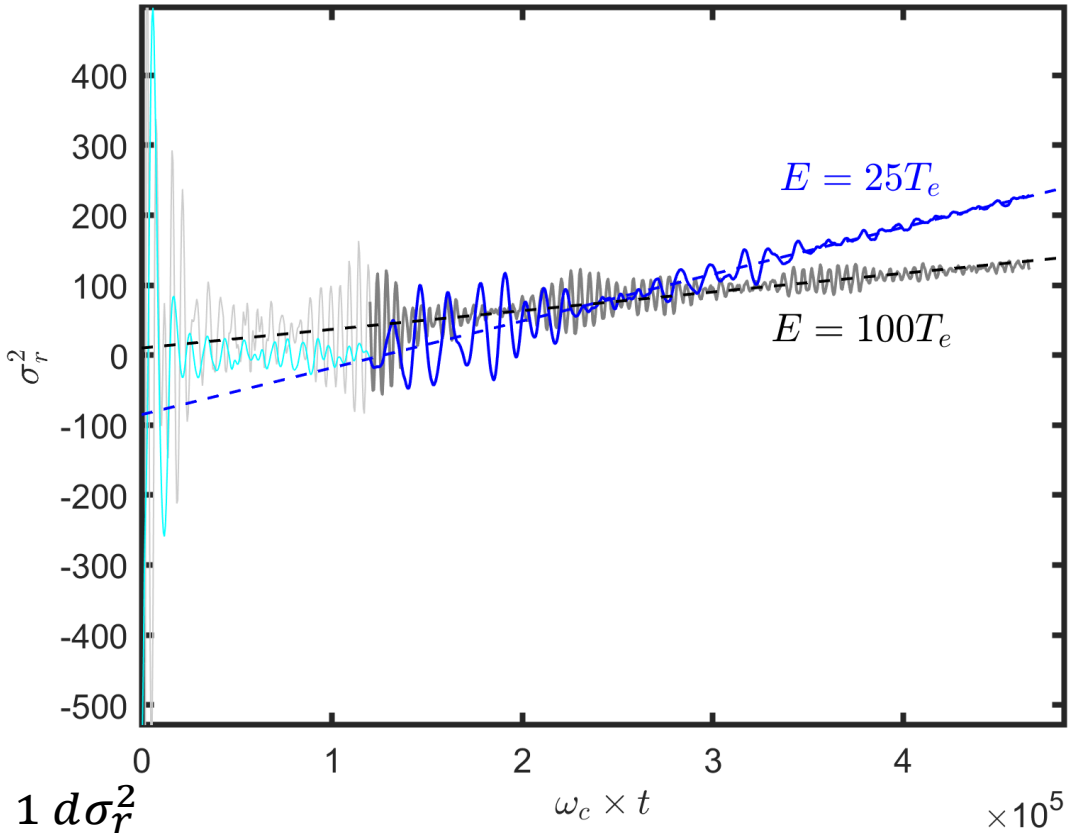

Possible reasons for the observed scaling

- Particles with $\lambda < -0.6$ (counter-passing) and $-0.3 < \lambda < 0$ (trapped close to the prompt losses region) are lost.
- The energy remains almost constant $\omega - n_2\Omega_2 - n_3\Omega_3 \approx n_2\Omega_2 - n_3\Omega_3 = 0$
  - Presence of resonances for the turbulent modes that can lead to the observed losses.
- Further analyses are required to assess the diffusive nature of the transport
  - For small energies, the PDF of displacements exhibits a Gaussian behaviour
  - For larger energies, the PDF departs from a Gaussian
  - Superdiffusion occurs when turbulent structures are relatively static with respect to the ions beyond a given threshold in turbulence amplitude [Gustafson PRL 2012]

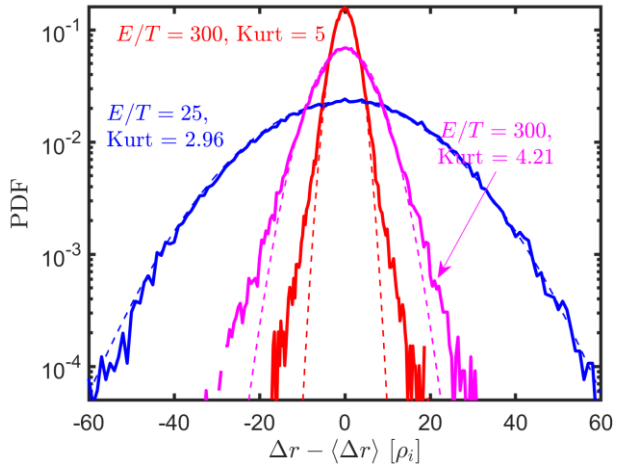

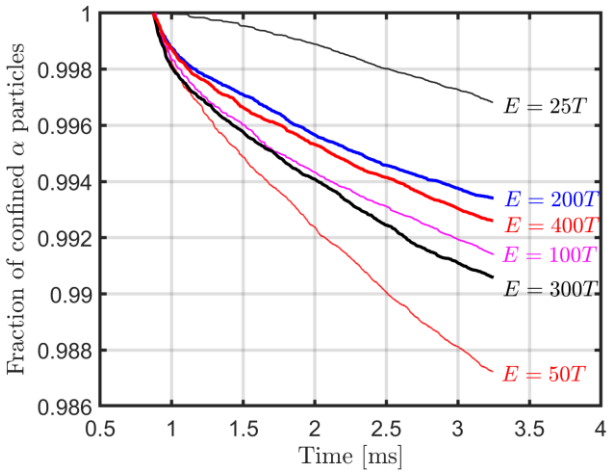

Different transport mechanisms of EP

Energetic particles = high energy → Collisions are rare

- ✓ Neoclassical transport is reduced ($D < 0.1 m^2/s$)

If 3 invariants → prompt losses = only possibility of « transport »

- ✓ Particles whose orbits intercept the wall (first orbit losses)

If < 3 invariants → transport

- ✓ Enhanced prompt losses (by small perturbations or small kicks)
- ✓ Convective resonant or non resonant transport
- ✓ Diffusive and non-diffusive (anomalous) transport
  - ➢ Several modes → Interaction between linear resonances
  - ➢ One mode → overlap of higher order resonances
    - Fractional resonances (large amplitude) [Kramer PRL2012]
    - Integer resonances (small amplitude) interacting with trapping cone [Zarzoso JPP2020]